
EDGERAZOR: A Lightweight Framework for Large Language Models via Mixed-Precision Quantization-Aware Distillation

Shu-Hao Zhang^{1,2} Le-Tong Huang^{1,2} Xiang-Sheng Deng^{1,2}
Xin-Yi Zou³ Chen Wu³ Nan Li³ Shao-Qun Zhang^{1,2,✉}

¹ State Key Laboratory of Novel Software Technology, Nanjing University, Nanjing 210023, China

² School of Intelligent Science and Technology, Nanjing University, Suzhou 215163, China

³ Microsoft AI, Beijing 100080, China

{zhangsh, zhangsq}@lamda.nju.edu.cn

Abstract

Recent years have witnessed an increasing interest in deploying Large Language Models (LLMs) on resource-constrained devices, among which quantization has emerged as a promising lightweight technique that converts full-precision model weights and activations into lower-bit formats. Existing weight quantization approaches can be roughly divided into three categories: Post-Training Quantization (PTQ) that calibrates quantized parameters on a small dataset without retraining but suffers from severe performance degradation below 4-bit, Quantization-Aware Training (QAT) that searches low-bit parameters using surrogate gradients but demands substantial computational resources, and Quantization-Aware Distillation (QAD) that integrates QAT with knowledge transfer from a full-precision teacher but manually selects features to distill and relies heavily on teacher-specific data. In this paper, we propose EDGERAZOR, a lightweight framework for LLMs with mixed-precision and extremely low-bit weight quantization. The EDGERAZOR framework contains three novel modules: Mixed-Precision Quantization-Aware Distillation for the fine-grained control of precision, Adaptive Feature Distillation that derives an n -bit student from its 16-bit teacher based on the most informative layers, and Entropy-Aware KL Divergence on both human-annotated and distilled datasets, whose forward-reverse balance is determined solely by the entropy of the teacher’s output distribution. Empirical investigations of EDGERAZOR are conducted on base, instruction-tuned, and multimodal LLMs. Notably, EDGERAZOR with 1.88-bit surpasses all contenders with the 3-bit precision, especially outperforms the leading 2-bit PTQ methods by 11.3 points, within a 4-10 \times lower training budget than the leading QAT approach. EDGERAZOR delivers higher compression ratios at all bit widths; 1.58-bit Qwen3-0.6B reduces storage from 1.41 GB to 0.28 GB while accelerating decoding by 15.1 \times relative to the 16-bit baseline. The distinctive feature of EDGERAZOR lies in the deep integration of quantization and distillation, with underlying optimizations specifically designed for resource-constrained scenarios; the code is available at github.com/zhangsq-nju/EdgeRazor.

1 Introduction

Large language models (LLMs) have become a hot topic in various domains, driven by the scaling law that model performance improves predictably with increasing model size, dataset size, and training computation. As empirical scaling laws drive the development of models expanding from

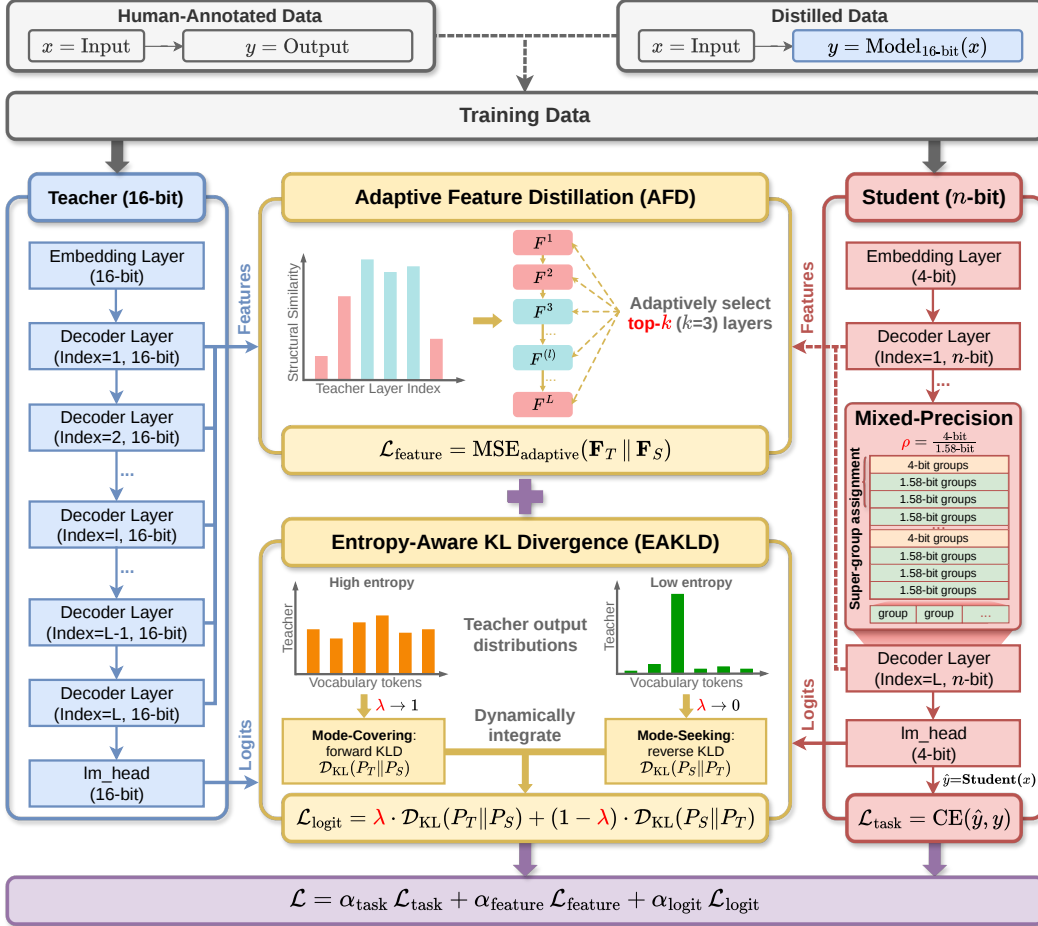


Figure 1: Overview of the EDGERAZOR framework. A 16-bit teacher guides an n -bit mixed-precision student through a joint objective of task-specific cross-entropy, AFD, and EAKLD.

sub-billion [36] to hundreds of billions of parameters [1, 52], a compelling demand has emerged for the lightweight deployment of LLMs on resource-constrained devices, where limited storage, memory, and computational capacity impose stringent constraints that full-precision models struggle to satisfy [57]. In recent years, quantization has emerged as a promising lightweight technique that converts full-precision model weights and activations into lower-bit formats [60]. A promising quantization method is expected to satisfy several prerequisites, including high performance, deployability on resource-constrained hardware, and a feasible training overhead [42].

Three main paradigms have been explored for LLM quantization: Post-Training Quantization (PTQ), Quantization-Aware Training (QAT), and Quantization-Aware Distillation (QAD). PTQ calibrates quantized parameters on a small dataset without retraining [15, 29], while suffering from severe performance degradation at lower bit-widths, as calibration alone is insufficient to compensate for the quantization error accumulated across Transformer layers [11]. QAT learns low-bit parameters using surrogate gradients [3], while executing dataset-driven gradient updates that directly fit target tasks to preserve performance below 4-bit, where PTQ methods collapse. Nevertheless, the training cost of QAT is substantial, including training from scratch and fine-tuning from pre-trained models [34, 46]. QAD integrates QAT with knowledge transfer from a full-precision teacher to alleviate the prohibitive training cost of QAT [33]. However, QAD methods typically rely on heuristic approaches for pre-specifying which teacher layers to supervise [51], which neither generalize across architectures nor guarantee optimality [47], and limit the forward KLD and reverse KLD switching criterion exclusively to teacher-distilled data [12], which precludes flexible data recipes that combine human-annotated and externally distilled corpora [48].

Existing quantization methods share an additional structural limitation: quantizing LLMs at uniform matrix-wise bit-widths. In contrast, mixed-precision quantization, which assigns heterogeneous

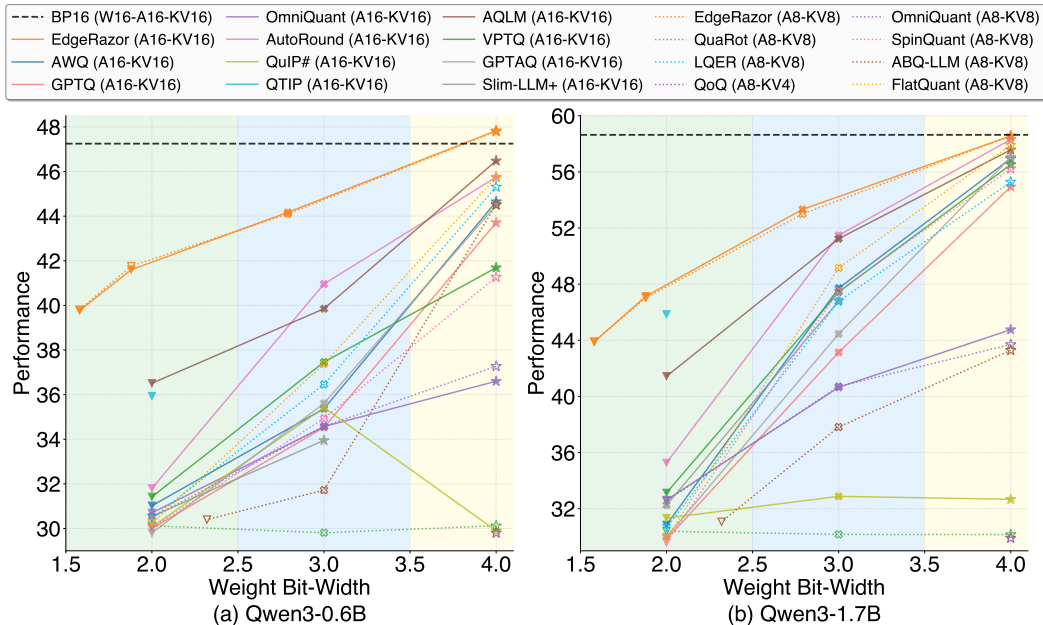


Figure 2: Average performance of quantized Qwen3 under EDGERAZOR and baselines.

bit-widths to different layers or weight groups according to their quantization sensitivity, is more adapted to real-world requirements. The motivation behind mixed-precision quantization is that not all parameters contribute equally to model quality [29]. Hence, forced compression of highly sensitive parameters would dominate the overall quantization error, whereas allocating additional bits to highly sensitive weight groups contributes to improving model performance [23, 29]. Meanwhile, the target average bit-width in practical deployment budgets seldom coincides with the discrete bit-widths offered by uniform-precision quantization [24], as a device whose memory can accommodate an average precision of 1.9-bit must choose between 1.58-bit, which results in over-compression, and 2-bit, which exceeds the budget. Mixed-precision quantization enables targeting an arbitrary average bit-width, thus effectively satisfying practical deployment budgets. Mixed-precision quantization has been extensively studied in PTQ methods, which suffer from severe performance gaps below 4-bit, while mixed-precision quantization with training remains unexplored.

In this paper, we propose EDGERAZOR, a lightweight framework for LLMs, as illustrated in Figure 1. The framework comprises three configurable modules: Mixed-Precision Quantization-Aware Distillation (MPQAD) that enables fine-grained control over the matrix-wise average bit-width, Adaptive Feature Distillation (AFD) that derives an n -bit student from its 16-bit teacher by adaptively selecting the most informative teacher layers for feature-level supervision, and Entropy-Aware KL Divergence (EAKLD) that weighs forward and reverse KLD solely by the entropy of the teacher’s output distribution, extending the logit distillation to both human-annotated and distilled datasets from the 16-bit teacher and other high-quality models. Driven by these techniques, EDGERAZOR significantly advances the performance of quantized LLMs across base, instruction-tuned, multimodal architectures as exemplified in Figure 2. On Qwen3-0.6B under weight-activation quantization, EDGERAZOR at 1.88-bit stably preserves core reasoning capabilities, surpassing all competing baselines evaluated at higher 3-bit precision and outperforming the state-of-the-art 2-bit PTQ baseline by 11.3 points across 14 domain-specific tasks. These performance gains generalize to other architectures such as base and multimodal LLMs with a training budget that is 4–10 \times lower than the leading QAT method. On the deployment end, our framework successfully translates theoretically optimal representations into tangible hardware efficiency. Executing the 1.58-bit Qwen3-0.6B via `llama.cpp` on an Apple M4 Pro CPU shrinks storage from 1.41 GB to 0.28 GB while achieving a 15.1 \times decoding speedup over the 16-bit baseline. We release EDGERAZOR as a modular open-source toolkit, which enables seamless integration of diverse quantization functions, distillation objectives, and plug-and-play training hooks, and supports various architectures across bit-widths from 4-bit down to 1.58-bit.

The rest of this paper is organized as follows. Section 2 presents related works. Section 3 proposes the EDGERAZOR framework for LLMs. Section 4 conducts comprehensive experiments. Section 5 concludes this work.

2 Related Works

Post-Training Quantization. PTQ compresses LLMs by calibrating quantized parameters on a small dataset without retraining. To maintain performance, existing methods employ local error compensation, such as weight adjustments through inverse Hessian approximation [15], activation-aware scaling and outlier smoothing [29, 49], or vector quantization space partitioning [44], successfully preserving near-lossless performance at 4-bit and above. Furthermore, mixed-precision PTQ attempts to optimize structural capacity by heuristically allocating heterogeneous bit-widths across distinct layers or groups [17, 23, 24], achieving better accuracy-efficiency trade-offs. Since calibration-driven strategies lack end-to-end gradient supervision, PTQ consistently suffers severe performance degradation when pushed below 4-bit, thereby limiting their viability for ultra-low-precision deployment [11].

Quantization-Aware Training. QAT maintains supervision to directly fit target tasks through executing dataset-driven gradient updates with surrogate gradients to bypass non-differentiable operations [3]. Existing methods typically adopt one of two paradigms: training natively quantized architectures entirely from scratch, as pioneered by BitNet [46], and fine-tuning from full-precision pre-trained models via block-wise reconstruction and optimized training budgets, exemplified by EfficientQAT [6] and ParetoQ [34], which significantly push the frontier of LLM compression to 2-bit or lower. Nevertheless, these gains inherently demand substantial computational resources and extensive corpus scales to converge [34, 46], rendering the paradigm prohibitively expensive for the downstream adaptations.

Quantization-Aware Distillation. QAD integrates QAT with knowledge transfer from a full-precision teacher to alleviate the prohibitive computational demands of QAT. Existing works align output logits and intermediate features, empowering sub-4-bit compression through data-free generation [33] and 1-bit structural decomposition [51]. Furthermore, recent advancements dynamically combine the standard mode-covering forward KLD [21] with the mode-seeking reverse KLD, utilizing metrics such as teacher prediction confidence [12], substantially improving zero-shot performance at lower bit-widths. However, existing QAD approaches remain bottlenecked by heuristic layer-selection strategies that struggle to generalize across architectures and lack guaranteed optimality for feature distillation [47], coupled with inflexible KLD switching criteria that strictly depend on teacher-distilled data, thereby restricting the use of diverse training recipes [48].

Open-Source Lightweight Ecosystem. The practical deployment of quantized LLMs relies heavily on the synergy between training and inference frameworks. On the inference front, mature engines such as llama.cpp and vLLM provide optimized low-bit execution for diverse hardware backends. On the training front, open-source frameworks for efficiently producing high-quality quantized LLMs remain fragmented. While PTQ benefits from mature, generalized toolkits, open-source QAT and QAD implementations [34, 12] are architecturally rigid. By tightly coupling quantization operators and distillation objectives to specific models without modular abstractions, they severely hinder plug-and-play extensibility and custom modifications.

3 EDGERAZOR

In this section, we propose EDGERAZOR, the workflow of which is illustrated in Figure 1. The EDGERAZOR framework consists of three novel modules: MPQAD that mixes 1.58-bit and 4-bit quantization precision by employing adjustable ratios in Subsection 3.1, AFD that aligns intermediate representations between student and teacher models by dynamically identifying the most informative layers rather than manually pre-specifying which layers to supervise in Subsection 3.2, and EAKLD that relies on the teacher’s output distribution to integrate forward and reverse KLD in Subsection 3.3. The overall training objective combines the low-bit student’s task-specific cross-entropy loss $\mathcal{L}_{\text{task}}$ with the two distillation losses

$$\mathcal{L} = \alpha_{\text{task}} \mathcal{L}_{\text{task}} + \alpha_{\text{feature}} \mathcal{L}_{\text{feature}} + \alpha_{\text{logit}} \mathcal{L}_{\text{logit}}, \quad (1)$$

where $\mathcal{L}_{\text{feature}}$ and $\mathcal{L}_{\text{logit}}$ correspond to AFD and EAKLD, respectively, and α_{task} , α_{logit} , α_{feature} are balancing coefficients.

3.1 Mixed-Precision Quantization-Aware Distillation

We adopt the per-group symmetric quantization for both weights and activations. Let $\mathbf{W} \in \mathbb{R}^{d_{\text{out}} \times d_{\text{in}}}$ denote a weight matrix and $\mathbf{X} \in \mathbb{R}^{d_{\text{in}} \times L}$ denote the corresponding activation matrix, where L is the sequence length. Given a group size G , we partition \mathbf{W} and \mathbf{X} along the input dimension into $J = d_{\text{in}}/G$ groups per output channel to get $\mathbf{W}^G \in \mathbb{R}^{d_{\text{out}} \times J}$ and $\mathbf{X}^G \in \mathbb{R}^{J \times L}$. The j -th group of the i -th output channel is defined as $\mathbf{W}_{i,j}^G = \mathbf{W}[i, jG : (j+1)G] \in \mathbb{R}^G$, with $W_{i,j,k}^G$ denoting its k -th element. Similarly, the j -th input-channel group for token l is defined as $\mathbf{X}_{j,l}^G = \mathbf{X}[jG : (j+1)G, l] \in \mathbb{R}^G$. Each group is independently quantized to n -bit through a symmetric quantization function applicable to both weights and activations,

$$Q_{n\text{-bit}}(\mathbf{W}_{i,j}) = \begin{cases} \text{clip}\left(\left\lfloor \frac{\mathbf{W}_{i,j}^G}{s_{i,j}} \right\rfloor, -1, 1\right) \text{ with } s_{i,j} = \max\left(\frac{\beta}{G} \sum_k |W_{i,j,k}^G|, \epsilon\right), & \text{if } n = 1.58 \\ \left\lfloor \frac{\mathbf{W}_{i,j}^G}{s_{i,j}} \right\rfloor \text{ with } s_{i,j} = \max\left(\frac{\max_k |W_{i,j,k}^G|}{2^{n-1} - 1}, \epsilon\right), & \text{if } n \in \{4, 8\} \end{cases} \quad (2)$$

where $\lfloor \cdot \rfloor$ denotes rounding to the nearest integer, $s_{i,j}$ is the scaling factor, β is a tunable scaling coefficient for ternarization, and ϵ is a small constant that prevents division by zero. The 1.58-bit branch, as $\log_2 3 \approx 1.58$, quantizes each weight to the ternary set $\{-1, 0, +1\}$, with the scaling factor derived from the group mean absolute value. The n -bit branch, where $n \in \{4, 8\}$, quantizes weights to the symmetric integer range such as $[-7, 7]$ for 4-bit and $[-127, 127]$ for 8-bit, with the scaling factor determined by the group-wise maximum absolute value.

Building on the above quantization function and the QAD paradigm, we propose MPQAD to determine the target bit-width. Note that activation groups are uniformly quantized to 8-bit under weight-activation quantization or retained at 16-bit under weight-only quantization. Specifically, MPQAD assigns a tunable parameter $\rho \in (0, 1)$ indicating the proportion of rows assigned to 4-bit, allocating the remaining $1 - \rho$ fraction to 1.58-bit. We organize this assignment into a regular repeating super-group pattern: every $\lfloor 1/\rho \rfloor$ consecutive rows of quantized groups along the input dimension form one super-group, wherein one row is quantized to 4-bit and the remainder to 1.58-bit. For instance, setting $\rho = 1/8$ places one 4-bit row followed by seven 1.58-bit rows within each super-group, culminating in an effective bit-width of roughly 1.88-bit. Since every super-group maintains this identical internal configuration, tuning ρ yields fine-grained, smooth control over the fractional bit-width. Then, under super-group assignment, each output element $Y_{i,l}$ is computed as

$$Y_{i,l} = \mathbf{W}_{i,\cdot}^G \cdot \mathbf{X}_{\cdot,l}^G = \sum_{j=0}^{J-1} \underbrace{s_{i,j}^W \cdot s_{j,l}^X}_{\textcircled{1}} \cdot \underbrace{Q_{n\text{-bit}}(\mathbf{W}_{i,j}^G)^\top Q_{8\text{-bit}}(\mathbf{X}_{j,l}^G)}_{\textcircled{2}}, \quad (3)$$

where $s_{i,j}^W$ and $s_{j,l}^X$ represent the floating-point scaling factors recovered from the per-group scales of weights and activations, respectively, which are multiplied together to form the combined scaling factor $\textcircled{1}$, and $\textcircled{2}$ is a low-bit integer dot product between the quantized weight and activation groups. This factorization is crucial for inference acceleration, as the integer arithmetic in $\textcircled{2}$ can be offloaded to efficient kernels on resource-constrained hardware.

The architectural design of this periodic super-group assignment fundamentally resolves the inherent restrictions of QAT and QAD. Unlike PTQ methods that statically preserve sensitive output channels [29, 23], quantization with training continuously updates weights, causing the optimal salience to shift correspondingly. By assigning precision along the input dimension, our mixed-precision layout ensures that every token accumulates an exact ρ fraction of 4-bit contributions, thereby effectively decoupling model performance from unpredictable salience fluctuations. Furthermore, because activation outliers are known to emerge sporadically across input channels [20], the interleaved super-group inherently functions as an evenly spaced high-precision buffer. This uniform distribution of average precision mitigates clustered quantization errors more effectively than segregated or random assignments. Beyond algorithmic stability, this deterministic, repeating structure aligns with hardware execution granularities, ensuring coalesced memory access and maximizing throughput for low-level kernel deployment.

3.2 Adaptive Feature Distillation

We propose AFD to adaptively identify the most informative layers for each input using a structural-similarity-based importance metric computed from the teacher. The core observation behind AFD is that consecutive transformer layers do not contribute equally to the overall feature transformation [43]. Certain layers induce substantial directional changes, whereas others leave the representation largely unchanged and contribute comparatively little new information. We explicitly quantify this structural similarity using cosine similarity to assess representational transformation, as the angular divergence between high-dimensional contextual embeddings inherently captures semantic and structural transformations [14]. To quantify this transformation across layers, we compute the mean cosine similarity between the outputs of adjacent teacher layers across all n positions in the sequence,

$$c_l = \frac{1}{n} \sum_{t=1}^n \cos\left(\mathbf{F}_{T,t}^{(l)}, \mathbf{F}_{T,t}^{(l-1)}\right), \quad l = 1, 2, \dots, L, \quad (4)$$

where $\mathbf{F}_{T,t}^{(l)} \in \mathbb{R}^d$ denotes the teacher’s features within a training batch at layer l and position t , and $\mathbf{F}_{T,t}^{(0)}$ corresponds to the output of the embedding layer. A low value of c_l indicates that layer l substantially transforms the representation direction and therefore carries a larger share of the model’s effective computation. We select the k layers with the lowest scores as the distillation targets,

$$\mathcal{S} = \arg \min_{S \subseteq \{1, \dots, L\}, |S|=k} \sum_{l \in S} c_l. \quad (5)$$

where \mathcal{S} is the set containing selected layers. The feature distillation loss is then defined over this adaptively selected set \mathcal{S} as

$$\mathcal{L}_{\text{feature}} = \text{MSE}_{\text{adaptive}}(\mathbf{F}_T \| \mathbf{F}_S) = \frac{1}{|\mathcal{S}|} \sum_{l \in \mathcal{S}} \frac{1}{|\mathcal{V}| \cdot d} \sum_{t \in \mathcal{V}} \left\| \mathbf{F}_{T,t}^{(l)} - \mathbf{F}_{S,t}^{(l)} \right\|_2^2, \quad (6)$$

where $\mathbf{F}_{S,t}^{(l)}$ is the corresponding student features and \mathcal{V} is the set of valid token positions excluding padding. By restricting the feature distillation loss to \mathcal{S} , AFD concentrates the gradient signal on the layers undergoing the most aggressive intermediate transformations. This critically prevents substantial quantization errors from propagating and amplifying through subsequent nonlinear computations. By leveraging structural similarity scores, AFD achieves optimal input-adaptive layer supervision while avoiding the prohibitive cost of searching over layer combinations.

3.3 Entropy-Aware KL Divergence

In logit distillation, the direction of KLD is used to align the student distribution P_S with the teacher distribution P_T . The forward KLD $\mathcal{D}_{\text{KL}}(P_T \| P_S)$ is zero-avoiding, preferentially inducing mode-covering behavior when the teacher spreads probability across multiple plausible tokens. Conversely, the reverse KLD $\mathcal{D}_{\text{KL}}(P_S \| P_T)$ is zero-forcing, inducing mode-seeking behavior that is more effective when the teacher’s confidence concentrates heavily on a few tokens [48].

To optimally harness both behaviors, we propose EAKLD, which dynamically interpolates between two objectives using a mixing coefficient λ . This coefficient is derived by evaluating the entropy of the teacher’s output distribution. The logit distillation loss and the mixing coefficient are defined as

$$\begin{aligned} \mathcal{L}_{\text{logit}} = \mathcal{D}_{\text{EAKLD}}(P_T \| P_S) &= \lambda \underbrace{\mathcal{D}_{\text{KL}}(P_T \| P_S)}_{\text{forward KLD}} + (1 - \lambda) \underbrace{\mathcal{D}_{\text{KL}}(P_S \| P_T)}_{\text{reverse KLD}}, \\ \text{with } \lambda &= \mathbb{E}_{(x,y) \sim \mathbb{D}} \left[\frac{1}{|y|} \sum_{i=1}^{|y|} \frac{\min\left(H(P_T(x, y_{<i})), \log k\right)}{\log k} \right], \end{aligned} \quad (7)$$

where \mathbb{D} is the data within a training batch, $|y|$ is the number of tokens in the response sequence, and $H(P_T(x, y_{<i}))$ denotes the entropy of the teacher’s predictive distribution at position i conditioned on the input x and the preceding tokens $y_{<i}$. Specifically, the entropy is formulated as

$$H(P_T(x, y_{<i})) = - \sum_{v \in \mathcal{V}} P_T(v | x, y_{<i}) \log P_T(v | x, y_{<i}), \quad (8)$$

where \mathcal{V} is the vocabulary set, and the denominator $\log k$ represents the maximum entropy of a k -uniform distribution. When the teacher disperses probability evenly among candidates, the entropy increases, causing λ to enlarge and adaptively strengthen the forward KLD to encourage mode-covering. Conversely, when the teacher places high confidence on dominant tokens, yielding a small $H(P_T)$, λ decays, thereby prioritizing the reverse KLD for precise mode-seeking. Furthermore, tuning the hyperparameter k deterministically alters the upper-bound entropy, acting as a single lever to adjust the entire dataset’s aggregate tendency toward either divergence strategy.

By adapting logit distillation exclusively from the entropy, EAKLD captures the full shape of the teacher’s uncertainty rather than relying on localized top- k probability statistics in BitDistiller [12]. Furthermore, it entirely obviates the need for distilled labels, supporting training corpora comprising both human-annotated and externally distilled responses.

4 Experiments

In this section, we conduct comprehensive experiments to validate the effectiveness and efficiency of the proposed EDGERAZOR framework along with its three modules.

4.1 Configurations

We equip the EDGERAZOR framework with four models: MobileLLM-350M [34] as the base LLM, Qwen3-0.6B and Qwen3-1.7B [52] as the instruction-tuned LLMs, and Qwen2.5-Omni-7B [50] as the multimodal LLM.

Table 1: Overview of datasets used for training.

#	Datasets	Subsets	Split	Data Sizes
1	BAAI/Infinity-Instruct [25]	7M_domains	train	7.45M
2	BAAI/Infinity-Instruct	Gen	train	1.4M
3	allenai/tulu-v3.1-mix-preview-4096-OLMoE	–	train	0.61M
4	a-m-team/AM-DeepSeek-R1-Distilled-1.4M [56]	am_0.5M+am_0.9M	train	1.4M
5	Mixed Downstream Datasets [4, 8, 9, 38, 39, 53]	–	train	0.1M
6	BAAI/Infinity-Instruct	7M_core	train	1.48M
7	HuggingFaceM4/TGIF [27]	–	train	10K

Training Data. Table 1 lists all training corpora, and Table 2 provides the training datasets used for each LLM. For the three text LLMs in non-reasoning mode, we assemble roughly 11 million instruction-response pairs from a mixture of human-annotated and distilled sources. The distilled portion comprises 1.4 million DeepSeek-R1 samples, from which chain-of-thought traces are removed. We also include the training splits of six downstream commonsense tasks, which together account for approximately 0.1 million examples. Crucially, all distilled samples originate from external models rather than the 16-bit teacher, so the EDGERAZOR framework does not rely on self-distilled corpora. For Qwen2.5-Omni-7B, we convert 10K GIF animations from the TGIF dataset to 30 FPS MP4 clips and distill video-understanding outputs from the 16-bit teacher.

Table 2: Hyperparameters for EDGERAZOR across diverse LLMs and bit-widths. The #Dataset column refers to the dataset indices in Table 1 as “1–5” denotes mixed datasets #1 through #5.

Models	ρ	Bit-Widths	LRs	LR Schedulers	Warmup Ratios	Epochs	Steps	# Datasets	Batch Sizes	α_{task}	α_{feature}	α_{logit}
Qwen3-0.6B	1.00	4	2e-05	Constant	0.05	-	2k	1–5	1024	0.05	0.50	2.00
	0.50	2.79	2e-05	Constant	0.05	1	-	1–5	1024	0.10	0.10	2.00
	0.125	1.88	2e-05	Constant	0.05	1	-	1–5	1024	0.10	0.10	2.00
	0	1.58	2e-05	Constant	0.05	1	-	1–5	1024	0.10	0.10	2.00
Qwen3-1.7B	1.00	4	2e-05	Constant	0.05	-	2k	1–5	1536	0.05	0.50	2.00
	0.50	2.79	2e-05	Constant	0.05	2	-	1–5	1536	0.10	0.10	2.00
	0.125	1.88	2e-05	Constant	0.05	2	-	1–5	1536	0.10	0.10	2.00
	0	1.58	2e-05	Constant	0.05	2	-	1–5	1536	0.10	0.10	2.00
MobileLLM-350M	1.00	4	2e-05	Cosine	0.01	2	-	5+6	1920	0.50	0.10	2.00
	0.50	2.79	2e-05	Cosine	0.01	4	-	5+6	1920	0.50	0.10	2.00
	0.125	1.88	2e-05	Cosine	0.01	5	-	5+6	1920	0.50	1.00	4.00
	0	1.58	2e-05	Cosine	0.01	5	-	5+6	1920	0.50	1.00	4.00
Qwen2.5-Omni-7B	1.00	4	5e-06	Cosine	0.01	2	-	7	64	0.10	0.20	2.00

Table 3: Overview of evaluation benchmarks used for EDGERAZOR.

Categories	Tasks	N-shot	Output Types	Metrics
Commonsense	ARC-e [9]	0-shot	Log-likelihood	Acc_norm
	ARC-c [9]	0-shot	Log-likelihood	Acc_norm
	HellaSwag [53]	0-shot	Log-likelihood	Acc_norm
	BoolQ [8]	0-shot	Log-likelihood	Acc
	PIQA [4]	0-shot	Log-likelihood	Acc_norm
	Winogrande [38]	0-shot	Log-likelihood	Acc
	SIQA [39]	0-shot	Log-likelihood	Acc
	OpenBookQA [37]	0-shot	Log-likelihood	Acc_norm
Truthfulness	TruthfulQA2 [30]	0-shot	Log-likelihood	Acc
	Ethics [18]	0-shot	Log-likelihood	Acc
Knowledge	MMLU [19]	0-shot	Log-likelihood	Acc
Instruction Following	IF-Eval [58]	0-shot	Generation	Prompt Strict Acc
Math	GSM8K [10]	5-shot	Log-likelihood	Acc
Code	HumanEval [5]	0-shot	Generation	Pass@1
Video Understanding	Video-MME [16]	0-shot	Generation	Acc
	MLVU [59]	0-shot	Generation	Acc

Hyperparameters. All training is performed on 8 NVIDIA A100-80 GB GPUs. We adopt per-group symmetric quantization throughout. The group size is 256 for the Qwen3 models and 64 for MobileLLM-350M and Qwen2.5-Omni-7B. To cover 99.99% of all parameters, the decoder layers are quantized to n -bit, while the embedding layer and language modeling head remain at 4-bit. Setting the 4-bit group proportion ρ to 1, 1/2, 1/8, and 0 deterministically yields matrix-wise average bit-widths of 4, 2.79, 1.88, and 1.58, respectively. The full set of training hyperparameters is detailed in Table 2. Models are optimized via AdamW with specific learning rates and schedules. We fix the small constant $\epsilon = 1e^{-5}$, the ternary scaling coefficient $\beta=2.0$, the number of AFD layers $k_{AFD}=3$, and the EAKLD entropy reference $k_{EAKLD}=16$ across all experiments.

Contenders and Evaluation. We compare against a comprehensive suite of state-of-the-art PTQ and QAT baselines, including GPTQ [15], OmniQuant [40], AWQ [29], AQLM [13], BiLLM [22], QuIP# [44], AutoRound [7], VPTQ [32], QTIP [45], ARB-LLM [28], GPTAQ [26], Slim-LLM+ [23], Q-Palette [24], LQER [55], QuaRot [2], ABQ-LLM [54], SpinQuant [35], QoQ [31], FlatQuant [41], EfficientQAT [6], and ParetoQ [34]. For distillation-level ablations, we isolate and compare our proposed EAKLD module against the CAKLD introduced in the QAD method BitDistiller [12] and our proposed AFD module against conventional feature distillation.

Table 3 summarizes the evaluation protocols. We prioritize domain-specific tasks over generic perplexity to reflect the concrete reasoning and generation capabilities of diverse LLMs. The text LLMs are benchmarked across 14 metrics, including commonsense reasoning, truthfulness, knowledge, instruction following, mathematics, and code generation, using the `lm_eval` library v0.4.9.1. The Qwen2.5-Omni-7B model is separately evaluated on two video understanding tasks using the `lmms_eval` library v0.5.0. To substantiate real-world deployment efficiency, we benchmark inference on an Apple M4 Pro CPU using `llama.cpp`.

4.2 Evaluation on n -bit Base LLMs

MobileLLM-350M. We select MobileLLM-350M as a representative base LLM. Tables 4 and 5 present the training budgets and results on quantized MobileLLM-350M. EDGERAZOR achieves the highest average performance at every bit-width while maintaining a moderate training budget.

Existing PTQ methods degrade severely on this tiny base LLM. Under the W-16-16 setting, AutoRound and QTIP yield average scores of only 31–33 regardless of bit-width, and FlatQuant drops from 40.40 at 4-bit to 30.82 at 2-bit. In contrast, EDGERAZOR achieves 41.86 at 4-bit and 39.02 at 1.88-bit under the same setting, significantly surpassing the best PTQ results.

Table 4: Training budget and average performance of QAT methods on MobileLLM-350M. The training budget is reported in tokens consumed during training.

Models	W-A-KV	Group Sizes	Training Budget (↓)	Average Performance (↑)
ParetoQ	4-16-16	channel	10B	<u>40.96</u>
ParetoQ	3-16-16	channel	10B	<u>40.24</u>
ParetoQ	2-16-16	channel	30B	<u>38.99</u>
ParetoQ	1.58-16-16	channel	30B	<u>38.00</u>
EfficientQAT	4-16-16	64	33M	40.89
EfficientQAT	3-16-16	64	33M	39.27
EfficientQAT	2-16-16	64	33M	36.24
EDGERAZOR	4-8-8	256	<u>1.2B</u>	41.86
EDGERAZOR	2.79-8-8	64	<u>2.4B</u>	40.62
EDGERAZOR	1.88-8-8	64	<u>3.1B</u>	39.02
EDGERAZOR	1.58-8-8	64	3.1B	38.12

Table 5: Performance of quantization methods on MobileLLM-350M across available bit-widths. **Bold** and underlined values indicate the best and second-best average performance.

Models	W-A-KV	ARC-e	ARC-c	HellaS.	BoolQ	PIQA	WinoG.	SIQA	OBQA	Tr.QA2	Ethics	MMLU	GSM8K	HumanE.	Average (↑)
MobileLLM-350M	16-16-16	64.94	35.49	52.87	58.96	70.84	56.35	40.79	40.20	37.44	53.98	23.52	0.00	0.00	41.18
AutoRound	4-16-16	26.39	29.69	25.79	61.71	50.33	48.78	33.62	27.60	48.14	43.60	26.90	0.00	0.00	32.50
AutoRound	3-16-16	25.72	29.27	25.81	61.90	50.33	49.80	33.78	27.00	47.78	43.59	27.00	0.00	0.00	32.46
AutoRound	2-16-16	25.88	29.27	25.86	60.00	49.95	51.62	33.16	26.20	47.95	46.53	27.12	0.00	0.00	32.58
QTIP	2-16-16	26.35	28.24	26.40	37.83	49.08	50.59	35.16	24.60	49.21	56.67	22.97	0.00	0.00	31.32
FlatQuant	4-8-8	61.95	34.73	51.72	58.93	70.84	53.75	40.33	39.00	38.01	52.24	23.56	0.15	0.00	40.40
FlatQuant	3-8-8	61.07	31.91	48.43	55.44	68.39	53.12	39.51	35.20	39.24	45.23	24.74	0.08	0.00	38.64
FlatQuant	2-8-8	31.44	22.27	27.19	44.71	51.74	47.59	34.60	25.40	49.22	43.53	23.03	0.00	0.00	30.82
ParetoQ	4-16-16	64.23	38.14	53.13	58.32	71.55	56.20	40.33	38.00	37.04	50.73	24.78	0.08	0.00	40.96
ParetoQ	3-16-16	62.75	33.28	51.24	60.92	70.95	56.75	39.82	39.00	37.00	46.39	25.02	0.00	0.00	40.24
ParetoQ	2-16-16	57.66	32.59	46.95	63.03	69.31	56.67	40.43	35.20	36.25	43.40	24.88	0.45	0.00	<u>38.99</u>
ParetoQ	1.58-16-16	56.10	29.95	43.68	61.62	67.30	54.30	39.30	36.40	38.82	43.34	23.05	0.15	0.00	38.00
EfficientQAT	4-16-16	63.68	35.67	51.73	58.47	70.73	56.75	40.74	38.40	37.11	54.07	24.16	0.00	0.00	40.89
EfficientQAT	3-16-16	61.53	33.11	49.45	60.89	69.04	53.75	39.66	36.80	37.66	45.35	22.24	0.00	0.00	39.27
EfficientQAT	2-16-16	49.92	27.05	39.29	61.77	63.49	50.91	37.56	29.60	42.50	46.05	22.93	0.00	0.00	36.24
EDGERAZOR	4-16-16	69.19	36.26	51.91	62.26	70.40	56.20	40.74	37.40	37.96	57.41	25.00	0.53	0.00	41.94
EDGERAZOR	2.79-16-16	65.87	32.68	45.98	61.71	68.82	56.27	40.02	35.00	38.97	56.53	24.27	0.76	0.00	<u>40.53</u>
EDGERAZOR	1.88-16-16	61.20	28.75	40.76	58.23	66.59	55.01	39.51	33.00	40.98	56.22	25.03	0.53	0.00	38.91
EDGERAZOR	1.58-16-16	58.63	26.19	38.95	58.07	65.29	53.04	39.30	32.20	41.97	56.26	24.12	0.53	0.00	<u>38.04</u>
EDGERAZOR	4-8-8	69.11	35.84	51.82	62.60	70.35	56.20	40.58	37.40	37.90	57.21	24.66	0.45	0.00	41.86
EDGERAZOR	2.79-8-8	65.99	32.68	45.99	62.11	68.55	56.51	40.07	35.20	39.05	56.51	24.41	0.99	0.00	40.62
EDGERAZOR	1.88-8-8	61.36	29.18	40.86	58.23	66.92	55.49	39.56	33.20	40.95	56.13	24.97	0.38	0.00	39.02
EDGERAZOR	1.58-8-8	58.67	26.19	38.92	58.04	65.23	53.83	39.25	32.00	42.03	56.33	24.19	0.83	0.00	38.12

Among QAT methods, EDGERAZOR consistently outperforms both ParetoQ and EfficientQAT despite evaluation under a stricter quantization configuration that additionally quantizes activations and KV cache to 8-bit. At 4-bit, EDGERAZOR reaches 41.86, exceeding the FP16 baseline of 41.18, ParetoQ at 40.96, and EfficientQAT at 40.89. At the 3-bit level, EDGERAZOR attains 40.62 at 2.79-bit, surpassing ParetoQ and EfficientQAT at 3-bit by 0.38 and 1.35, respectively. At the 2-bit level, EDGERAZOR achieves 39.02 at 1.88-bit, matching ParetoQ at 2-bit while outperforming EfficientQAT at 2-bit by 2.78 points. Notably, these gains come at a substantially lower training budget. As reported in Table 4, EDGERAZOR consumes 1.2B–3.1B training tokens, roughly 4–10× fewer than the 10B–30B tokens required by ParetoQ. Although EfficientQAT requires only 33M tokens, its performance falls behind at every bit-width, with the gap widening at lower precision. The experimental results demonstrate that EDGERAZOR achieves the best effectiveness–efficiency trade-off, surpassing ParetoQ in accuracy with a 4–10× lower training budget.

4.3 Evaluation on n -bit Instruction-Tuned LLMs

Qwen3-0.6B. Table 6 reports weight-only quantization results on Qwen3-0.6B. EDGERAZOR achieves the highest average performance at every bit-width, with a margin consistently widening as precision drops. At 4-bit, it reaches 47.83, slightly above the FP16 baseline of 47.35, while the second-best AQLM trails at 46.48. The advantage becomes more significant at lower bit-widths. At 2.79-bit, EDGERAZOR achieves 44.17, surpassing AutoRound, the strongest 3-bit PTQ baseline

Table 6: Average performance of weight-only quantization methods on Qwen3-0.6B across available bit-widths. **Bold** and underlined values indicate the best and second-best average performance. Superscripts denote exact bit-widths for non-standard configurations.

Methods	Average Performance (\uparrow)				
	W16-A16-KV16	W4-A16-KV16	W3-A16-KV16	W2-A16-KV16	W1.58-A16-KV16
BF16	47.35	–	–	–	–
GPTQ	–	43.71	34.53	30.00	–
OmniQuant	–	36.60	34.57	30.70	–
AWQ	–	44.65	35.37	31.02	–
AQLM	–	<u>46.48</u>	39.85	<u>36.51</u>	–
BiLLM	–	–	–	–	29.98 ^{W1.06}
QuIP#	–	29.90	35.42	30.07	–
AutoRound	–	45.75	<u>40.96</u>	31.80	–
VPTQ	–	41.69	<u>37.46</u>	31.42	–
QTIP	–	–	–	35.94	–
ARB-LLM	–	–	–	–	30.77 ^{W1.00}
GPTAQ	–	44.49	35.61	29.80	–
Slim-LLM+	–	–	33.95	30.54	–
Q-Palette	–	40.97	37.55 ^{W3.25}	30.66	<u>30.81</u> ^{W1.75}
EDGERAZOR	–	47.83	44.17 ^{W2.79}	41.60 ^{W1.88}	39.77

Table 7: Average performance of weight-activation quantization methods on Qwen3-0.6B across available bit-widths. **Bold** and underlined values indicate the best and second-best average performance. Superscripts denote exact bit-widths for non-standard configurations.

Methods	Average Performance (\uparrow)				
	W16-A16-KV16	W4-A8-KV8	W3-A8-KV8	W2-A8-KV8	W1.58-A8-KV8
BF16	47.35	–	–	–	–
OmniQuant	–	37.27	34.58	<u>30.49</u>	–
LQER	–	45.31	36.46	30.46	–
QuaRot	–	30.12	29.81	30.12	–
ABQ-LLM	–	44.52	31.72	30.40 ^{W2.32}	–
SpinQuant	–	41.27	34.93	30.04	–
QoQ	–	29.80 ^{KV4}	–	–	–
FlatQuant	–	<u>45.74</u>	<u>37.38</u>	30.23	–
EDGERAZOR	–	47.80	44.10 ^{W2.79}	41.76 ^{W1.88}	39.81

with a score of 40.96, by 3.21 points. At 1.88-bit, EDGERAZOR attains 41.60, exceeding AQLM’s second-best 2-bit result of 36.51 by over 5 points. Notably, EDGERAZOR at the 2-bit level surpasses every baseline evaluated at 3-bit, effectively preserving roughly one additional bit of precision in terms of model quality. This trend persists at 1.58-bit, where EDGERAZOR still scores 39.77, leading Q-Palette’s 1.75-bit result by 8.96 points and even surpassing the best PTQ 2-bit result, AQLM, by 3.26 points. Per-task results, listed in Table 16, reveal that most 2-bit baselines collapse to near-zero on challenging tasks such as GSM8K and HumanEval, whereas EDGERAZOR retains meaningful scores of 25.09 and 23.17, respectively. These results indicate the effectiveness of EDGERAZOR for preserving reasoning and code-generation capabilities under extreme compression.

Table 7 presents results under weight-activation quantization with 8-bit activations and KV cache. EDGERAZOR achieves the highest average score at every configuration, and its advantage over the strongest baseline also grows as weight precision decreases. At 4-bit, EDGERAZOR averages 47.80, surpassing the runner-up FlatQuant at 45.74 by 2.06 points. This result also exceeds the full-precision BF16 reference of 47.35, and differs from EDGERAZOR’s own weight-only score of 47.83 by only 0.03 points, suggesting that 8-bit activation and KV cache quantization introduce no additional error. At 3-bit, EDGERAZOR reaches 44.10 at an effective 2.79-bit weight representation, outperforming FlatQuant’s 3-bit result of 37.38 by 6.72 points. At 2-bit, all baselines fall to roughly 30 in average performance, with OmniQuant reaching the highest at 30.49, while EDGERAZOR at effective 1.88-bit achieves 41.76, retaining over 11 points of advantage and again surpassing every

Table 8: Average performance of weight-only quantization methods on Qwen3-1.7B across available bit-widths. **Bold** and underlined values indicate the best and second-best average performance. Superscripts denote exact bit-widths for non-standard configurations.

Methods	Average Performance (\uparrow)				
	W16-A16-KV16	W4-A16-KV16	W3-A16-KV16	W2-A16-KV16	W1.58-A16-KV16
BF16	58.64	–	–	–	–
GPTQ	–	54.94	43.14	29.82	–
OmniQuant	–	44.76	40.65	32.62	–
AWQ	–	56.95	47.71	30.85	–
AQLM	–	57.57	51.24	41.44	–
BiLLM	–	–	–	–	29.15 ^{W1.04}
QuIP#	–	32.67	32.88	31.33	–
AutoRound	–	<u>58.31</u>	<u>51.48</u>	35.27	–
VPTQ	–	<u>56.52</u>	<u>47.44</u>	33.13	–
QTIP	–	–	–	<u>45.85</u>	–
ARB-LLM	–	–	–	–	30.61 ^{W1.00}
GPTAQ	–	57.05	44.45	29.98	–
Slim-LLM+	–	–	46.80	32.26	–
Q-Palette	–	49.77	47.66	33.06	<u>30.92</u> ^{W1.75}
EDGERAZOR	–	58.56	53.33 ^{W2.79}	47.14 ^{W1.88}	43.89

baseline evaluated at 3-bit. Furthermore, EDGERAZOR’s joint-quantization performances differ from their weight-only counterparts by at most a fraction of a point across all bit-widths, confirming its robustness to activation and KV cache quantization. The per-task details in Table 17 also reveal that several baselines fail on challenging benchmarks such as GSM8K and HumanEval at bit-widths below 4-bit, while EDGERAZOR at 1.88-bit preserves scores of 25.09 and 23.17 on these two tasks.

Qwen3-1.7B. Table 8 reports weight-only quantization results on Qwen3-1.7B, where EDGERAZOR achieves the best average performance at every bit-width. At 4-bit, it scores 58.56, 0.08 below the BF16 reference of 58.64 and ahead of AutoRound at 58.31, the second-best PTQ method. At the 3-bit level, EDGERAZOR reaches 53.33 at 2.79-bit, outperforming the second-best AutoRound’s 3-bit score of 51.48 by 1.85 points. The separation grows substantially at the 2-bit level, where most baselines fall below an average of 36. Only QTIP at 45.85 and AQLM at 41.44 remain competitive. EDGERAZOR at 1.88-bit nevertheless leads both, scoring 47.14. This result is competitive with the 3-bit tier, surpassing five of nine baselines at that precision and falling within one point of AWQ’s 3-bit average performance of 47.71. At 1.58-bit, EDGERAZOR still attains 43.89, exceeding all 2-bit baselines except QTIP and leading the second-best below-2-bit method Q-Palette at 1.75-bit by 12.97 points. Per-task results in Table 18 reveal that seven of ten baselines at 2-bit produce zero scores on both GSM8K and HumanEval, and only QTIP retains non-zero performances of 27.37 and 21.95, whereas EDGERAZOR at 1.88-bit preserves scores of 36.39 and 39.63, respectively. The overall pattern mirrors the Qwen3-0.6B findings, including near-lossless 4-bit quantization, consistent margins at lower bit-widths, and robust preservation of reasoning and code-generation capabilities.

Table 9 extends the evaluation to joint weight-activation quantization with 8-bit activations and KV cache. EDGERAZOR leads at every bit-width. Its 4-bit average of 58.57 lies within 0.08 of the BF16 reference and 0.67 above FlatQuant’s 57.90. At 2.79-bit, EDGERAZOR reaches 53.00, exceeding FlatQuant’s 3-bit result of 49.16 by 3.84 and SpinQuant’s 47.51 by 5.49. The gap widens at the 2-bit level, where the best baseline is OmniQuant at 32.56, and EDGERAZOR at 1.88-bit achieves 47.03. EDGERAZOR at 1.58-bit still achieves 43.91, leading all PTQ baselines at 2-bit. Comparing with Table 8, the added activation and KV cache quantization cost EDGERAZOR no more than 0.33 points at any bit-width, consistent with the robustness observed on Qwen3-0.6B. Per-task results in Appendix Table 19 show that all six baselines at 2-bit score zero on both GSM8K and HumanEval, while EDGERAZOR at 1.88-bit preserves 37.53 and 40.85 on these two tasks.

4.4 Evaluation on 4-bit Multimodal LLMs

Qwen2.5-Omni-7B. To validate generalization beyond text-only LLMs, we select Qwen2.5-Omni-7B as a representative multimodal LLM and evaluate it on the Video-MME and MLVU benchmarks

Table 9: Average performance of weight-activation quantization methods on Qwen3-1.7B across available bit-widths. **Bold** and underlined values indicate the best and second-best average performance. Superscripts denote exact bit-widths for non-standard configurations.

Methods	Average Performance (\uparrow)				
	W16-A16-KV16	W4-A8-KV8	W3-A8-KV8	W2-A8-KV8	W1.58-A8-KV8
BF16	58.65	–	–	–	–
OmniQuant	–	43.70	40.71	<u>32.56</u>	–
LQER	–	55.28	46.78	30.63	–
QuaRot	–	30.16	30.17	30.39	–
ABQ-LLM	–	43.29	37.82	31.07 ^{W2.32}	–
SpinQuant	–	56.22	47.51	29.62	–
QoQ	–	29.91 ^{KV4}	–	–	–
FlatQuant	–	<u>57.90</u>	<u>49.16</u>	29.87	–
EDGERAZOR	–	58.57	53.00 ^{W2.79}	47.03 ^{W1.88}	43.91

Table 10: Performance of weight-only quantization methods on 4-bit Qwen2.5-Omni-7B. **Bold** and underlined values indicate the best and second-best average performance.

Methods	W-A-KV	Quantized Modules		Video-MME	MLVU	Average (\uparrow)
		Vision Encoder	LLM Decoder			
Qwen2.5-Omni-7B	16-16-16	×	×	62.81	48.01	55.41
AWQ	4-16-16	×	✓	61.78	47.40	<u>54.59</u>
GPTQ	4-16-16	×	✓	60.51	48.06	<u>54.29</u>
EDGERAZOR	4-16-16	✓	✓	62.22	48.82	55.52

for video understanding. For the quantization configurations, AWQ and GPTQ quantize only the decoder layers in the LLM backbone, whereas EDGERAZOR additionally quantizes the vision encoder, embedding layer, and the language modeling head.

As reported in Table 10, EDGERAZOR averages 55.52 despite quantizing a substantially larger portion of the model, marginally exceeding the BF16 baseline of 55.41 and outperforming AWQ and GPTQ by 0.93 and 1.23 points. On MLVU, EDGERAZOR reaches 48.82, which is 0.81 above the unquantized score and may reflect a mild regularization effect of mixed-precision allocation on long-context video reasoning. On Video-MME, EDGERAZOR at 62.22 incurs only a 0.59-point drop from full precision, whereas GPTQ loses 2.30. These results confirm that EDGERAZOR transfers to multimodal architectures without any degradation, achieving effective lossless 4-bit quantization.

4.5 Ablation Studies on Feature and Logit Distillation

Table 11: Configurations for the ablation studies of EDGERAZOR.

Methods	Feature Distillation		Logit Distillation		
	Adaptive	Fixed	EAKLD	CAKLD [12]	forward KLD
EDGERAZOR _{A+E}	✓	×	✓	×	×
EDGERAZOR _{A+C}	✓	×	×	✓	×
EDGERAZOR _{F+E}	×	✓	✓	×	×
EDGERAZOR _{F+F}	×	✓	×	×	✓

In the previous sections, the experimental results demonstrate the effectiveness of EDGERAZOR’s mixed-precision quantization with training through achieving consistent performance improvements with lower average bit-widths. In this section, we conduct ablation studies on Qwen3-0.6B to validate the effectiveness of two distillation modules: AFD and EAKLD. As shown in Table 11, we design four configurations: EDGERAZOR_{A+E} employs the full configuration with AFD and EAKLD; EDGERAZOR_{A+C} replaces EAKLD with CAKLD introduced by BitDistiller [12]; EDGERAZOR_{F+E} replaces adaptive layer selection with fixed layer selection covering low, middle, and high decoder layers; and EDGERAZOR_{F+F} combines forward KLD with fixed feature distillation. All configurations

Table 12: Ablation studies of quantization methods based on EDGERAZOR. The quantized layers, including decoder, embedding, and lm_head, are all 2.19-bit (25% 4-bit and 75% 1.58-bit).

Methods	W-A-KV	ARC-e	ARC-c	HellaS.	BoolQ	PIQA	WinoG.	SIQA	OBQA	Tr.QA2	Ethics	MMLU	IFEval	GSM8K	HumanE.	Average (↑)
EDGE _{A+E}	2.19-16-16	50.17	29.44	34.21	63.88	62.89	50.83	37.00	29.80	43.59	48.45	31.77	38.82	24.64	24.39	40.71
EDGE _{A+E}	2.19-8-8	49.24	28.67	34.28	63.98	61.86	50.43	36.69	29.80	44.14	47.12	31.71	39.19	22.90	21.95	40.14
EDGE _{A+C}	2.19-16-16	52.27	27.82	33.59	65.05	62.46	50.20	37.92	28.00	44.54	43.29	27.05	40.30	20.39	21.34	39.59
EDGE _{A+C}	2.19-8-8	52.31	27.47	33.70	64.65	62.19	50.51	37.77	27.80	44.59	43.29	27.13	40.30	20.24	22.56	39.61
EDGE _{F+E}	2.19-16-16	49.03	27.05	34.33	59.57	62.51	51.46	38.28	30.20	45.34	53.63	27.88	36.97	27.37	20.12	40.27
EDGE _{F+E}	2.19-8-8	47.77	26.96	34.02	59.33	61.86	52.09	38.13	30.60	44.98	53.22	27.89	35.67	27.60	18.90	39.93
EDGE _{F+F}	2.19-16-16	49.15	26.11	30.04	52.29	63.38	51.70	38.23	29.00	45.85	55.86	29.13	36.04	22.59	20.12	39.25
EDGE _{F+F}	2.19-8-8	48.99	26.11	33.24	51.83	62.89	51.38	38.13	28.40	45.92	55.77	28.98	37.15	21.15	23.17	39.51

Table 13: Ablation studies of quantization methods based on EDGERAZOR. The decoder layers are 1.88-bit (12.5% 4-bit and 87.5% 1.58-bit), while the embedding and lm_head layers are 4-bit.

Methods	W-A-KV	ARC-e	ARC-c	HellaS.	BoolQ	PIQA	WinoG.	SIQA	OBQA	Tr.QA2	Ethics	MMLU	IFEval	GSM8K	HumanE.	Average (↑)
EDGE _{A+E}	1.88-16-16	51.22	27.73	34.21	66.91	63.66	53.35	38.43	27.60	43.80	55.92	28.78	42.51	25.09	23.17	41.60
EDGE _{A+E}	1.88-8-8	51.47	27.99	34.22	66.85	63.49	53.04	38.02	27.40	43.88	55.92	29.56	44.55	25.09	23.17	41.76
EDGE _{A+C}	1.88-16-16	49.20	27.56	34.64	65.05	61.75	53.67	39.36	30.00	44.35	54.72	30.90	39.56	23.05	19.51	40.95
EDGE _{A+C}	1.88-8-8	49.16	27.47	34.50	64.95	61.75	54.06	39.20	29.40	44.47	54.80	30.59	37.34	22.21	21.95	40.85
EDGE _{F+E}	1.88-16-16	48.57	26.45	33.60	58.65	61.53	53.20	39.30	29.40	43.67	56.46	33.21	40.67	20.77	20.12	40.40
EDGE _{F+E}	1.88-8-8	48.15	25.94	33.75	58.50	60.83	52.72	38.54	29.40	43.50	56.44	33.33	41.04	19.86	21.34	40.24
EDGE _{F+F}	1.88-16-16	47.90	27.39	34.23	61.83	61.43	52.49	38.23	26.80	47.87	54.12	26.46	39.37	20.55	18.90	39.83
EDGE _{F+F}	1.88-8-8	48.06	26.96	34.30	61.77	61.37	51.93	38.38	26.60	47.53	52.13	25.99	39.74	20.92	20.12	39.70

are evaluated under two weight quantization settings, 2.19-bit in Table 12, and 1.88-bit integrated with 4-bit in Table 13, each paired with both 16-bit and 8-bit activation and KV cache.

Comparing EDGE_{A+E} with EDGE_{A+C} reveals the effect of the logit distillation objective. EDGE_{A+E} consistently outperforms EDGE_{A+C}, achieving improvements of 1.12 and 0.53 points in average performance at 2.19-bit, and 0.65 and 0.91 points at 1.88-bit. This confirms that EAKLD provides more effective logit-level supervision than CAKLD for transferring knowledge from the 16-bit teacher to the quantized student. Comparing EDGE_{A+E} with EDGE_{F+E} demonstrates the contribution of AFD. EDGE_{A+E} surpasses EDGE_{F+E} by 0.44 and 0.21 points at 2.19-bit, and by 1.20 and 1.52 points at 1.88-bit. The larger gains under stricter quantization suggest that adaptive layer selection becomes increasingly important as the bit-width decreases, where accurately identifying the most informative layers for feature alignment is more critical. Comparing EDGE_{F+E} with EDGE_{F+F}, both of which adopt fixed feature distillation, further demonstrates the advantage of EAKLD over standard forward KLD. EDGE_{F+E} outperforms EDGE_{F+F} by 1.02 and 0.42 points at 2.19-bit, and by 0.57 and 0.54 points at 1.88-bit. Combined with the first comparison, this confirms the consistent superiority of EAKLD over adaptive and conventional logit distillation. Across all configurations, EDGE_{A+E} achieves the highest average performance, validating that the proposed combination of EAKLD and AFD achieves the most effective quantization-aware distillation within the EDGERAZOR framework.

4.6 Efficiency

We select Qwen3-0.6B as a representative to evaluate efficiency from two perspectives: theoretical compression and practical inference performance on edge hardware. For theoretical compression, the metrics are quantized layers, quantization proportion, and compression ratio. For practical inference performance, the metrics are storage, memory, prefilling throughput, and decoding throughput.

Compression. EDGERAZOR achieves substantially higher quantization proportion and compression ratios than existing methods at every bit-width due to additional quantization on the embedding layer and the language modeling head. Table 14 compares three quantization paradigms on Qwen3-0.6B: per-group EDGERAZOR with group size 256, per-group methods such as AutoRound, GPTQ, and EfficientQAT with group size 128, and per-channel methods such as QuaRot, FlatQuant, and ParetoQ. The fundamental distinction lies in quantization coverage. EDGERAZOR quantizes almost all model parameters, reaching a quantization proportion of 99.99%. However, other methods only quantize decoder layers and leave 26.11% of weights in full precision. This difference translates directly into compression advantages. At 4-bit, EDGERAZOR achieves a 3.94× compression ratio, compared

Table 14: Compression comparison of various quantization methods.

Models	Group Sizes	Quantized Layers			Bit-Widths	Quantization	Compression
		Decoder	Emb	Lm_head		Proportions (\uparrow)	Ratios (\uparrow)
Qwen3-0.6B	–	–	–	–	16	–	1.00 \times
EDGERAZOR	256	✓	✓	✓	4	99.99%	3.94\times
	256	✓	✓	✓	2.79	99.99%	5.05\times
	256	✓	✓	✓	1.88	99.99%	6.40\times
	256	✓	✓	✓	1.58	99.99%	7.03\times
Other Methods	128	✓	×	×	4	73.89%	2.21 \times
	128	✓	×	×	3	73.89%	2.47 \times
	128	✓	×	×	2	73.89%	2.78 \times
	128	✓	×	×	1.58	73.89%	2.94 \times
Other Methods	channel	✓	×	×	4	73.89%	2.24 \times
	channel	✓	×	×	3	73.89%	2.50 \times
	channel	✓	×	×	2	73.89%	2.83 \times
	channel	✓	×	×	1.58	73.89%	2.99 \times

Table 15: Efficiency comparison of EDGERAZOR n -bit, llama.cpp BF16 and PTQ on Qwen3-0.6B.

Models	W-A-KV	Weight Types	KV Types	Storage (GB \downarrow)	Memory (GB \downarrow)	Prefilling (tokens/s \uparrow)	Decoding (tokens/s \uparrow)
Qwen3-0.6B	16-16-16	BF16	BF16	1.406	1.747	335.91	21.60
Llama.cpp PTQ	4-8-8	Q4_K	Q8_0	0.451	0.767	717.05	233.47
EDGERAZOR	4-8-8	Q4_0	Q8_0	0.437	0.751	1275.25	270.25
EDGERAZOR	2.79-8-8	No support	–	–	–	–	–
EDGERAZOR	1.88-8-8	No support	–	–	–	–	–
Llama.cpp PTQ	2-8-8	Q2_K	Q8_0	0.323	0.639	704.7	224.80
EDGERAZOR	1.58-8-8	TQ1_0	Q8_0	0.255	0.490	665.92	292.05
EDGERAZOR	1.58-8-8	TQ2_0	Q8_0	0.275	0.509	659.63	325.19

to 2.21 \times for per-group and 2.24 \times for per-channel methods. The difference widens at lower bit-widths. At 1.58-bit, EDGERAZOR attains 7.03 \times compression compared to 2.94 \times and 2.99 \times for the two baselines. These results confirm that comprehensive parameter coverage is a prerequisite for maximizing compression on small-scale LLMs, which tend to be deployed on edge devices.

Inference. We further validate practical efficiency using llama.cpp on an Apple M4 Pro chip under the CPU-only configuration with Metal and BLAS backends, 10 threads, and a batch size of 4096, and measure storage, memory, and throughput for both prefilling (512 tokens) and decoding (512 tokens) stages. As shown in Table 15, the theoretical compression advantages of EDGERAZOR transfer faithfully to a real inference environment. EDGERAZOR consistently achieves the lowest storage and memory footprint at 4-bit and 1.58-bit precisions, matching the pattern of compression ratios calculated in Table 14.

At 4-bit, EDGERAZOR deployed with the Q4_0 format outperforms the llama.cpp built-in PTQ method Q4_K across all metrics, reducing storage from 0.451 GB to 0.437 GB and memory from 0.767 GB to 0.751 GB, while improving prefilling throughput from 717.05 to 1275.25 tokens/s and decoding throughput from 233.47 to 270.25 tokens/s. At 1.58-bit, EDGERAZOR with TQ1_0 and TQ2_0 formats reduces storage to 0.255 and 0.275 GB and memory to 0.490 and 0.509 GB, compared to 0.323 GB and 0.639 GB for Q2_K, while significantly improving decoding throughput to 292.05 and 325.19 tokens/s versus 224.80 tokens/s for Q2_K. The prefilling throughput of TQ1_0 665.92 and TQ2_0 659.63 is slightly lower than Q2_K 704.7 tokens/s due to more complex ternary packing.

Compared to the BF16 baseline, both configurations achieve substantial efficiency gains that are particularly relevant for edge deployment. EDGERAZOR at 4-bit reduces 3.2 \times storage and 2.3 \times memory, while improving prefilling and decoding throughput by 3.8 \times and 12.5 \times respectively. EDGERAZOR at 1.58-bit with TQ2_0 achieves even greater reductions of 5.1 \times in storage and 3.4 \times in memory, with prefilling and decoding throughput improvements of 2.0 \times and 15.1 \times respectively.

These gains bring the model size below 300 MB and peak memory below 510 MB, making deployment feasible on memory-constrained hardware such as mobile and IoT devices.

In Table 15, the two inference stages exhibit distinct throughput profiles due to different bottlenecks. Prefilling processes the full prompt as a batched GEMM, where weights are loaded once and reused across all input tokens, making the phase compute-bound. Q4_0 achieves the highest prefilling speed because its symmetric dequantization with a single scale per 32-weight block maps directly onto SIMD-vectorized kernels and fully utilizes the available compute. Decoding performs a GEMV for each generated token. Each weight is streamed from memory yet consumed only once, so bandwidth becomes the dominant constraint. TQ1_0 and TQ2_0 deliver the best decoding throughput, as their ternary packing compresses weights to about 1.7 and 2.1 effective bits-per-weight, reducing per-step memory traffic by 2 to 2.5 times relative to 4-bit formats. Despite being less compact, TQ2_0 decodes faster than TQ1_0 at 325.19 versus 292.05 tokens/s. TQ1_0 unpacks weights by base-3 arithmetic involving integer division and modulo, while TQ2_0 uses straightforward 2-bit masking and shifting.

5 Conclusions

In this paper, we propose EDGERAZOR, a lightweight framework for LLMs with three novel modules: MPQAD, AFD, and EAKLD. Extensive evaluations across base, instruction-tuned, and multimodal LLMs demonstrate the superior performance of EDGERAZOR under both weight-only and weight-activation quantization. Notably, for Qwen3-0.6B at an extreme 1.88-bit precision, EDGERAZOR not only outperforms the leading 2-bit PTQ baseline by a remarkable 11.3 points but also surpasses all existing 3-bit methods, effectively mitigating the catastrophic capability collapse typical of ultra-low-bit compression. Crucially, these gains are achieved with exceptional training efficiency, consuming 4–10× fewer tokens than the state-of-the-art QAT method. On the deployment front, the low-bit Qwen3-0.6B maximizes theoretical structural capacity by achieving a 99.99% quantization proportion, unlocking a striking 7.03× compression ratio at 1.58-bit. When deployed on an Apple M4 Pro CPU, the 1.58-bit Qwen3-0.6B drastically reduces storage from 1.41 GB to 0.28 GB and memory footprint from 1.75 GB to 0.51 GB. This structural compactness translates directly to exceptional inference acceleration. Compared to the 16-bit baseline, it achieves a 2.0× improvement in prefilling throughput, increasing from 335.91 tokens/s to 659.63 tokens/s, while delivering a massive 15.1× speedup in decoding throughput, surging from 21.60 tokens/s to 325.19 tokens/s.

6 Acknowledgement

Shao-Qun Zhang is the corresponding author, supported by the Natural Science Foundation of China (62406138) and the Natural Science Foundation of Jiangsu Province (BK20230782). This research was supported by the Fundamental and Interdisciplinary Disciplines Breakthrough Plan of the Ministry of Education of China (No. JYB2025XDXM118).

This research was performed during Shu-Hao Zhang’s internship at Microsoft AI, where the proposed EDGERAZOR framework was evaluated and deployed within the internal systems.

References

- [1] Josh Achiam, Steven Adler, Sandhini Agarwal, Lama Ahmad, Ilge Akkaya, Florencia Leoni Aleman, Diogo Almeida, Janko Altschmidt, Sam Altman, Shyamal Anadkat, et al. GPT-4 technical report. *arXiv preprint arXiv:2303.08774*, 2023.
- [2] Saleh Ashkboos, Amirkeivan Mohtashami, Maximilian L Croci, Bo Li, Pashmina Cameron, Martin Jaggi, Dan Alistarh, Torsten Hoefler, and James Hensman. QuaRot: Outlier-free 4-bit inference in rotated LLMs. In *Advances in Neural Information Processing Systems 37*, pages 100213–100240, 2024.
- [3] Yoshua Bengio, Nicholas Léonard, and Aaron Courville. Estimating or propagating gradients through stochastic neurons for conditional computation. *arXiv preprint arXiv:1308.3432*, 2013.
- [4] Yonatan Bisk, Rowan Zellers, Ronan Le Bras, Jianfeng Gao, and Yejin Choi. PIQA: Reasoning about physical commonsense in natural language. In *Proceedings of the 34th AAAI Conference on Artificial Intelligence*, pages 7432–7439, 2020.

- [5] Mark Chen, Jerry Tworek, Heewoo Jun, Qiming Yuan, Henrique Ponde De Oliveira Pinto, Jared Kaplan, Harri Edwards, Yuri Burda, Nicholas Joseph, Greg Brockman, et al. Evaluating large language models trained on code. *arXiv preprint arXiv:2107.03374*, 2021.
- [6] Mengzhao Chen, Wenqi Shao, Peng Xu, Jiahao Wang, Peng Gao, Kaipeng Zhang, Yu Qiao, and Ping Luo. EfficientQAT: Efficient quantization-aware training for large language models. In *Proceedings of the 63rd Annual Meeting of the Association for Computational Linguistics*, pages 10081–10100, 2025.
- [7] Wenhua Cheng, Weiwei Zhang, Haihao Shen, Yiyang Cai, Xin He, Lv Kaokao, and Yi Liu. Optimize weight rounding via signed gradient descent for the quantization of LLMs. In *Findings of the Association for Computational Linguistics: EMNLP 2024*, pages 11332–11350, 2024.
- [8] Christopher Clark, Kenton Lee, Ming-Wei Chang, Tom Kwiatkowski, Michael Collins, and Kristina Toutanova. BoolQ: Exploring the surprising difficulty of natural yes/no questions. In *Proceedings of the 2019 Conference of the North American Chapter of the Association for Computational Linguistics*, pages 2924–2936, 2019.
- [9] Peter Clark, Isaac Cowhey, Oren Etzioni, Tushar Khot, Ashish Sabharwal, Carissa Schoenick, and Oyvind Tafjord. Think you have solved question answering? Try ARC, the AI2 reasoning challenge. *arXiv preprint arXiv:1803.05457*, 2018.
- [10] Karl Cobbe, Vineet Kosaraju, Mohammad Bavarian, Mark Chen, Heewoo Jun, Lukasz Kaiser, Matthias Plappert, Jerry Tworek, Jacob Hilton, Reiichiro Nakano, et al. Training verifiers to solve math word problems. *arXiv preprint arXiv:2110.14168*, 2021.
- [11] Tim Dettmers and Luke Zettlemoyer. The case for 4-bit precision: K-bit inference scaling laws. In *Proceedings of the 40th International Conference on Machine Learning*, pages 7750–7774, 2023.
- [12] Dayou Du, Yijia Zhang, Shijie Cao, Jiaqi Guo, Ting Cao, Xiaowen Chu, and Ningyi Xu. BitDistiller: Unleashing the potential of sub-4-bit LLMs via self-distillation. In *Proceedings of the 62nd Annual Meeting of the Association for Computational Linguistics*, pages 102–116, 2024.
- [13] Vage Egiazarian, Andrei Panferov, Denis Kuznedelev, Elias Frantar, Artem Babenko, and Dan Alistarh. Extreme compression of large language models via additive quantization. In *Proceedings of the 41st International Conference on Machine Learning*, pages 12284–12303, 2024.
- [14] Kawin Ethayarajh. How contextual are contextualized word representations? Comparing the geometry of BERT, ELMo, and GPT-2 embeddings. In *Proceedings of the 2019 Conference on Empirical Methods in Natural Language Processing*, pages 55–65, 2019.
- [15] Elias Frantar, Saleh Ashkboos, Torsten Hoefler, and Dan Alistarh. GPTQ: Accurate post-training quantization for generative pre-trained transformers. *arXiv preprint arXiv:2210.17323*, 2022.
- [16] Chaoyou Fu, Yuhan Dai, Yongdong Luo, Lei Li, Shuhuai Ren, Renrui Zhang, Zihan Wang, Chenyu Zhou, Yunhang Shen, Mengdan Zhang, et al. Video-MME: The first-ever comprehensive evaluation benchmark of multi-modal LLMs in video analysis. In *Proceedings of the IEEE/CVF Conference on Computer Vision and Pattern Recognition*, pages 24108–24118, 2025.
- [17] Ziyi Guan, Hantao Huang, Yupeng Su, Hong Huang, Ngai Wong, and Hao Yu. APTQ: Attention-aware post-training mixed-precision quantization for large language models. In *Proceedings of the 61st ACM/IEEE Design Automation Conference*, pages 1–6, 2024.
- [18] Dan Hendrycks, Collin Burns, Steven Basart, Andrew Critch, Jerry Li, Dawn Song, and Jacob Steinhardt. Aligning AI with shared human values. *arXiv preprint arXiv:2008.02275*, 2020.
- [19] Dan Hendrycks, Collin Burns, Steven Basart, Andy Zou, Mantas Mazeika, Dawn Song, and Jacob Steinhardt. Measuring massive multitask language understanding. *arXiv preprint arXiv:2009.03300*, 2020.
- [20] Jung Hwan Heo, Jeonghoon Kim, Beomseok Kwon, Byeongwook Kim, Se Jung Kwon, and Dongsoo Lee. Rethinking channel dimensions to isolate outliers for low-bit weight quantization of large language models. In *Proceedings of the 12th International Conference on Learning Representations*, pages 12744–12762, 2024.
- [21] Geoffrey Hinton, Oriol Vinyals, and Jeff Dean. Distilling the knowledge in a neural network. *arXiv preprint arXiv:1503.02531*, 2015.
- [22] Wei Huang, Yangdong Liu, Haotong Qin, Ying Li, Shiming Zhang, Xianglong Liu, Michele Magno, and Xiaojuan Qi. BiLLM: Pushing the limit of post-training quantization for LLMs. In *Proceedings of the 41st International Conference on Machine Learning*, pages 20023–20042, 2024.

- [23] Wei Huang, Haotong Qin, Yangdong Liu, Yawei Li, Qinshuo Liu, Xianglong Liu, Luca Benini, Michele Magno, Shiming Zhang, and Xiaojuan Qi. SliM-LLM: Saliency-driven mixed-precision quantization for large language models. In *Proceedings of the 42nd International Conference on Machine Learning*, pages 25672–25692, 2025.
- [24] Deokjae Lee and Hyun Oh Song. Q-Palette: Fractional-bit quantizers toward optimal bit allocation for efficient LLM deployment. *arXiv preprint arXiv:2509.20214*, 2025.
- [25] Jijie Li, Li Du, Hanyu Zhao, Bowen Zhang, Liangdong Wang, Boyan Gao, Guang Liu, and Yonghua Lin. Infinity Instruct: Scaling instruction selection and synthesis to enhance language models. *arXiv preprint arXiv:2506.11116*, 2025.
- [26] Yuhang Li, Ruokai Yin, Donghyun Lee, Shiting Xiao, and Priyadarshini Panda. GPTAQ: Efficient finetuning-free quantization for asymmetric calibration. In *Proceedings of the 42nd International Conference on Machine Learning*, pages 36690–36706, 2025.
- [27] Yuncheng Li, Yale Song, Liangliang Cao, Joel Tetreault, Larry Goldberg, Alejandro Jaimes, and Jiebo Luo. TGIF: A new dataset and benchmark on animated gif description. In *Proceedings of the IEEE Conference on Computer Vision and Pattern Recognition*, pages 4641–4650, 2016.
- [28] Zhiteng Li, Xianglong Yan, Tianao Zhang, Haotong Qin, Dong Xie, Jiang Tian, Zhongchao Shi, Linghe Kong, Yulun Zhang, and Xiaokang Yang. ARB-LLM: Alternating refined binarizations for large language models. In *Proceedings of the 13th International Conference on Learning Representations*, pages 93900–93912, 2025.
- [29] Ji Lin, Jiaming Tang, Haotian Tang, Shang Yang, Wei-Ming Chen, Wei-Chen Wang, Guangxuan Xiao, Xingyu Dang, Chuang Gan, and Song Han. AWQ: Activation-aware weight quantization for on-device LLM compression and acceleration. In *Proceedings of the 6th Conference on Machine Learning and Systems*, volume 6, pages 87–100, 2024.
- [30] Stephanie Lin, Jacob Hilton, and Owain Evans. TruthfulQA: Measuring how models mimic human falsehoods. In *Proceedings of the 60th Annual Meeting of the Association for Computational Linguistics*, pages 3214–3252, 2022.
- [31] Yujun Lin, Haotian Tang, Shang Yang, Zhekai Zhang, Guangxuan Xiao, Chuang Gan, and Song Han. QServe: W4A8KV4 quantization and system co-design for efficient LLM serving. In *Proceedings of the 7th Conference on Machine Learning and Systems*, 2025.
- [32] Yifei Liu, Jicheng Wen, Yang Wang, Shengyu Ye, Li Lina Zhang, Ting Cao, Cheng Li, and Mao Yang. VPTQ: Extreme low-bit vector post-training quantization for large language models. In *Proceedings of the 2024 Conference on Empirical Methods in Natural Language Processing*, pages 8181–8196, 2024.
- [33] Zechun Liu, Barlas Oguz, Changsheng Zhao, Ernie Chang, Pierre Stock, Yashar Mehdad, Yangyang Shi, Raghuraman Krishnamoorthi, and Vikas Chandra. LLM-QAT: Data-free quantization aware training for large language models. *arXiv preprint arXiv:2305.17888*, 2023.
- [34] Zechun Liu, Changsheng Zhao, Igor Fedorov, Bilge Soran, Dhruv Choudhary, Raghuraman Krishnamoorthi, Vikas Chandra, Yuandong Tian, and Tijmen Blankevoort. ParetoQ: Scaling laws in extremely low-bit LLM quantization. *arXiv preprint arXiv:2502.02631*, 2025.
- [35] Zechun Liu, Changsheng Zhao, Igor Fedorov, Bilge Soran, Dhruv Choudhary, Raghuraman Krishnamoorthi, Vikas Chandra, Yuandong Tian, and Tijmen Blankevoort. SpinQuant: LLM quantization with learned rotations. In *Proceedings of the 13th International Conference on Learning Representations*, pages 92009–92032, 2025.
- [36] Zechun Liu, Changsheng Zhao, Forrest Iandola, Chen Lai, Yuandong Tian, Igor Fedorov, Yunyang Xiong, Ernie Chang, Yangyang Shi, Raghuraman Krishnamoorthi, et al. MobileLLM: Optimizing sub-billion parameter language models for on-device use cases. In *Proceedings of the 41st International Conference on Machine Learning*, pages 31267–31289, 2024.
- [37] Todor Mihaylov, Peter Clark, Tushar Khot, and Ashish Sabharwal. Can a suit of armor conduct electricity? A new dataset for open book question answering. In *Proceedings of the 2018 Conference on Empirical Methods in Natural Language Processing*, pages 2381–2391, 2018.
- [38] Keisuke Sakaguchi, Ronan Le Bras, Chandra Bhagavatula, and Yejin Choi. WinoGrande: An adversarial Winograd schema challenge at scale. *Communications of the ACM*, 64(9):99–106, 2021.

- [39] Maarten Sap, Hannah Rashkin, Derek Chen, Ronan Le Bras, and Yejin Choi. Social IQa: Commonsense reasoning about social interactions. In *Proceedings of the 2019 Conference on Empirical Methods in Natural Language Processing*, pages 4463–4473, 2019.
- [40] Wenqi Shao, Mengzhao Chen, Zhaoyang Zhang, Peng Xu, Lirui Zhao, Zhiqian Li, Kaipeng Zhang, Peng Gao, Yu Qiao, and Ping Luo. OmniQuant: Omnidirectionally calibrated quantization for large language models. In *Proceedings of the 12th International Conference on Learning Representations*, pages 45472–45496, 2024.
- [41] Yuxuan Sun, Ruikang Liu, Haoli Bai, Han Bao, Kang Zhao, Yuening Li, Jiaxin Hu, Xianzhi Yu, Lu Hou, Chun Yuan, Xin Jiang, Wulong Liu, and Jun Yao. FlatQuant: Flatness matters for LLM quantization. In *Proceedings of the 42nd International Conference on Machine Learning*, pages 57587–57613, 2025.
- [42] Fuwen Tan, Royson Lee, Łukasz Dudziak, Shell Xu Hu, Sourav Bhattacharya, Timothy Hospedales, Georgios Tzimopoulos, and Brais Martinez. MobileQuant: Mobile-friendly quantization for on-device language models. In *Findings of the Association for Computational Linguistics: EMNLP 2024*, pages 9761–9771, 2024.
- [43] Ian Tenney, Dipanjan Das, and Ellie Pavlick. BERT rediscovers the classical NLP pipeline. In *Proceedings of the 57th Annual Meeting of the Association for Computational Linguistics*, pages 4593–4601, 2019.
- [44] Albert Tseng, Jerry Chee, Qingyao Sun, Volodymyr Kuleshov, and Christopher De Sa. QuIP#: Even better LLM quantization with hadamard incoherence and lattice codebooks. In *Proceedings of the 41st International Conference on Machine Learning*, pages 48630–48656, 2024.
- [45] Albert Tseng, Qingyao Sun, David Hou, and Christopher M De Sa. QTIP: Quantization with trellises and incoherence processing. In *Advances in Neural Information Processing Systems 37*, pages 59597–59620, 2024.
- [46] Hongyu Wang, Shuming Ma, Lingxiao Ma, Lei Wang, Wenhui Wang, Li Dong, Shaohan Huang, Huaijie Wang, Jilong Xue, Ruiping Wang, et al. BitNet: 1-bit pre-training for large language models. *Journal of Machine Learning Research*, 26(125):1–29, 2025.
- [47] Wenhui Wang, Furu Wei, Li Dong, Hangbo Bao, Nan Yang, and Ming Zhou. MiniLM: Deep self-attention distillation for task-agnostic compression of pre-trained transformers. In *Advances in Neural Information Processing Systems 33*, pages 5776–5788, 2020.
- [48] Taiqiang Wu, Chaofan Tao, Jiahao Wang, Runming Yang, Zhe Zhao, and Ngai Wong. Rethinking kullback-leibler divergence in knowledge distillation for large language models. In *Proceedings of the 31st International Conference on Computational Linguistics*, pages 5737–5755, 2025.
- [49] Guangxuan Xiao, Ji Lin, Mickael Seznec, Hao Wu, Julien Demouth, and Song Han. SmoothQuant: Accurate and efficient post-training quantization for large language models. In *Proceedings of the 40th International Conference on Machine Learning*, pages 38087–38099, 2023.
- [50] Jin Xu, Zhifang Guo, Jinzheng He, Hangrui Hu, Ting He, Shuai Bai, Keqin Chen, Jialin Wang, Yang Fan, Kai Dang, et al. Qwen2.5-omni technical report. *arXiv preprint arXiv:2503.20215*, 2025.
- [51] Yuzhuang Xu, Xu Han, Zonghan Yang, Shuo Wang, Qingfu Zhu, Zhiyuan Liu, Weidong Liu, and Wanxiang Che. OneBit: Towards extremely low-bit large language models. In *Advances in Neural Information Processing Systems 37*, pages 66357–66382, 2024.
- [52] An Yang, Anfeng Li, Baosong Yang, Beichen Zhang, Binyuan Hui, Bo Zheng, Bowen Yu, Chang Gao, Chengen Huang, Chenxu Lv, et al. Qwen3 technical report. *arXiv preprint arXiv:2505.09388*, 2025.
- [53] Rowan Zellers, Ari Holtzman, Yonatan Bisk, Ali Farhadi, and Yejin Choi. HellaSwag: Can a machine really finish your sentence? In *Proceedings of the 57th Annual Meeting of the Association for Computational Linguistics*, pages 4791–4800, 2019.
- [54] Chao Zeng, Songwei Liu, Yusheng Xie, Hong Liu, Xiaojian Wang, Miao Wei, Shu Yang, Fangmin Chen, and Xing Mei. ABQ-LLM: Arbitrary-bit quantized inference acceleration for large language models. In *Proceedings of the 39th AAAI Conference on Artificial Intelligence*, pages 22299–22307, 2025.
- [55] Cheng Zhang, Jianyi Cheng, George A Constantinides, and Yiren Zhao. LQER: Low-rank quantization error reconstruction for LLMs. In *Proceedings of the 41st International Conference on Machine Learning*, pages 58763–58779, 2024.

- [56] Han Zhao, Haotian Wang, Yiping Peng, Sitong Zhao, Xiaoyu Tian, Shuaiting Chen, Yunjie Ji, and Xiangang Li. 1.4 million open-source distilled reasoning dataset to empower large language model training. *arXiv preprint arXiv:2503.19633*, 2025.
- [57] Yue Zheng, Yuhao Chen, Bin Qian, Xiufang Shi, Yuanchao Shu, and Jiming Chen. A review on edge large language models: Design, execution, and applications. *ACM Computing Surveys*, 57(8):1–35, 2025.
- [58] Jeffrey Zhou, Tianjian Lu, Swaroop Mishra, Siddhartha Brahma, Sujoy Basu, Yi Luan, Denny Zhou, and Le Hou. Instruction-following evaluation for large language models. *arXiv preprint arXiv:2311.07911*, 2023.
- [59] Junjie Zhou, Yan Shu, Bo Zhao, Boya Wu, Zhengyang Liang, Shitao Xiao, Minghao Qin, Xi Yang, Yongping Xiong, Bo Zhang, et al. MLVU: Benchmarking multi-task long video understanding. In *Proceedings of the IEEE/CVF Conference on Computer Vision and Pattern Recognition*, pages 13691–13701, 2025.
- [60] Xunyu Zhu, Jian Li, Yong Liu, Can Ma, and Weiping Wang. A survey on model compression for large language models. *Transactions of the Association for Computational Linguistics*, 12:1556–1577, 2024.

A Details of Experimental Results

In Tables 16, 17, 18, and 19, we report the comprehensive per-task results underlying the average scores presented in the main text. Across all models and bit-widths, generation-intensive tasks such as GSM8K and HumanEval exhibit the most substantial degradation under aggressive quantization, often falling to near zero at 2-bit for baseline methods. In contrast, discriminative benchmarks such as ARC-e, BoolQ, and PIQA are considerably more resilient.

On these challenging tasks, including MMLU, IFEval, GSM8K, and HumanEval, EDGERAZOR consistently outperforms other low-bit methods by a clear margin, although a non-trivial gap relative to the 16-bit baseline persists at sub-3-bit precisions. These per-task results suggest that the novel modules in EDGERAZOR are particularly effective in preserving the knowledge required for complex reasoning and instruction following.

Table 16: Performance of weight-only quantization methods on Qwen3-0.6B across various bit-widths. **Bold** and underlined values indicate the best and second-best average performance.

Models	W-A-KV	ARC-e	ARC-c	HellaS.	BoolQ	PIQA	WinoG.	SIQA	OBQA	Tr-QA2	Ethics	MMLU	IFEval	GSM8K	HumanE.	Average (↑)
Qwen3-0.6B	16-16-16	56.02	34.04	47.23	64.04	67.36	56.04	39.20	31.20	42.84	47.70	40.12	58.41	41.54	37.20	47.35
GPTQ	4-16-16	52.78	32.85	45.10	61.71	65.18	55.56	41.15	31.00	44.89	49.67	33.86	53.05	26.23	18.90	43.71
GPTQ	3-16-16	36.91	25.60	38.66	60.18	60.66	53.67	38.54	28.80	43.48	44.84	26.45	24.95	0.61	0.00	34.53
GPTQ	2-16-16	24.87	25.26	26.43	42.63	51.41	53.43	33.83	27.00	47.60	54.33	24.72	8.50	0.00	0.00	30.00
OmniQuant	4-16-16	47.01	31.06	44.43	58.32	65.18	57.06	38.28	31.80	42.32	44.39	40.55	12.01	0.00	0.00	36.60
OmniQuant	3-16-16	44.61	26.02	38.94	63.36	61.81	54.62	36.90	29.40	43.81	43.25	30.56	10.72	0.00	0.00	34.57
OmniQuant	2-16-16	32.41	22.27	28.55	38.62	55.22	50.51	34.54	24.60	51.28	56.73	22.92	12.20	0.00	0.00	30.70
AWQ	4-16-16	52.15	31.91	45.36	61.56	65.45	54.22	37.62	31.00	39.34	46.07	40.62	56.56	33.97	29.27	44.65
AWQ	3-16-16	39.69	26.62	39.77	57.55	61.92	54.46	37.36	29.60	44.94	45.67	27.97	25.14	2.65	1.83	35.37
AWQ	2-16-16	25.17	26.71	26.22	61.62	51.31	51.46	33.52	26.60	48.12	45.77	26.89	10.91	0.00	0.00	31.02
AQLM	4-16-16	52.82	33.19	47.03	63.91	67.41	55.64	39.76	33.20	42.69	45.44	41.04	56.01	40.26	32.32	46.48
AQLM	3-16-16	50.42	29.18	43.13	64.19	64.47	56.43	39.56	31.60	41.97	44.42	31.28	44.73	15.85	0.61	39.85
AQLM	2-16-16	40.49	29.86	40.72	43.00	64.15	55.56	37.36	31.00	44.02	47.88	33.79	34.75	8.49	0.00	<u>36.51</u>
BiLLM	1.06-16-16	27.36	25.94	27.06	46.64	51.41	49.49	33.01	26.20	49.25	47.49	24.28	11.65	0.00	0.00	29.98
QuIP#	4-16-16	26.05	26.71	26.11	45.78	49.40	50.75	33.62	27.20	45.32	52.45	24.68	10.54	0.00	0.00	29.90
QuIP#	3-16-16	44.07	28.41	38.00	63.82	62.19	54.06	36.23	29.00	45.29	44.97	28.06	19.78	1.97	0.00	35.42
QuIP#	2-16-16	27.53	23.55	27.18	37.83	51.69	51.22	34.75	27.00	50.27	56.67	22.78	10.54	0.00	0.00	30.07
AutoRound	4-16-16	51.47	31.31	45.56	67.31	66.81	53.83	39.71	31.40	41.72	44.57	41.20	55.45	32.98	37.20	45.75
AutoRound	3-16-16	47.43	27.99	41.60	58.20	63.49	54.14	37.92	30.80	42.16	56.72	40.49	39.74	13.80	18.90	<u>40.96</u>
AutoRound	2-16-16	35.31	22.70	31.43	60.43	58.16	51.70	35.16	27.60	45.54	46.28	22.92	7.95	0.00	0.00	31.80
VPTQ	4-16-16	47.01	30.20	45.19	67.19	66.43	55.56	39.36	29.80	43.21	45.14	31.08	51.76	31.69	0.00	41.69
VPTQ	3-16-16	42.30	28.92	40.85	63.49	61.81	50.83	39.41	29.40	46.50	46.01	28.04	33.27	6.29	7.32	37.46
VPTQ	2-16-16	32.11	24.15	31.14	57.52	55.98	51.46	36.39	26.40	47.13	44.99	23.52	8.87	0.15	0.00	31.42
QTIP	2-16-16	44.99	27.30	39.79	65.93	62.24	55.80	38.74	29.60	43.33	45.59	23.17	23.48	3.26	0.00	35.94
ARB-LLM	1-16-16	28.37	25.51	29.30	46.36	53.05	49.49	34.08	26.20	47.61	54.66	23.71	12.38	0.00	0.00	30.77
GPTAQ	4-16-16	50.93	33.45	45.31	61.19	66.43	56.91	40.58	31.20	43.90	52.43	38.84	52.87	29.87	18.90	44.49
GPTAQ	3-16-16	40.87	26.28	39.93	60.34	61.26	54.70	38.64	29.40	43.30	47.20	29.07	26.25	1.29	0.00	35.61
GPTAQ	2-16-16	26.47	24.91	26.25	40.18	50.98	49.96	34.80	27.20	49.41	55.01	24.07	7.95	0.00	0.00	29.80
Slim-LLM+	3-16-16	42.13	25.09	38.52	62.94	61.48	53.99	36.44	29.60	44.81	43.41	27.78	3.33	5.76	0.00	33.95
Slim-LLM+	2-16-16	30.68	21.16	27.93	37.92	55.60	51.38	35.21	26.60	50.35	56.67	22.99	11.09	0.00	0.00	30.54
Q-Palette	4-16-16	52.23	31.74	45.22	49.79	65.40	53.83	39.87	30.80	43.55	55.79	35.59	30.68	0.00	39.02	40.97
Q-Palette	3.25-16-16	42.09	27.90	42.27	59.54	64.15	52.96	39.25	30.60	43.08	44.60	33.22	27.17	0.00	18.90	37.55
Q-Palette	2-16-16	29.92	23.63	28.44	60.95	52.88	48.86	33.67	25.40	45.89	46.39	24.18	9.06	0.00	0.00	30.66
Q-Palette	1.75-16-16	28.96	25.68	27.06	60.18	52.29	48.93	34.08	26.20	47.16	44.75	23.12	12.94	0.00	0.00	<u>30.81</u>
EDGE RAZOR	4-16-16	58.54	33.45	45.04	68.01	68.34	55.72	40.07	33.40	43.69	54.36	39.37	53.42	42.00	34.15	47.83
EDGE RAZOR	2.79-16-16	51.77	28.33	37.47	70.70	63.71	54.06	40.33	28.20	42.72	55.08	36.85	51.39	26.69	31.10	44.17
EDGE RAZOR	1.88-16-16	51.22	27.73	34.21	66.91	63.66	53.35	38.43	27.60	43.80	55.92	28.78	42.51	25.09	23.17	41.60
EDGE RAZOR	1.58-16-16	45.75	25.77	33.89	66.64	60.72	52.33	38.23	29.80	44.40	51.70	32.85	37.34	14.25	23.17	39.77

Table 17: Performance of weight-activation quantization methods on Qwen3-0.6B across various bit-widths. **Bold** and underlined values indicate the best and second-best average performance.

Models	W-A-KV	ARC-e	ARC-c	HellaS.	BoolQ	PIQA	WinoG.	SIQA	OBQA	TrQA2	Ethics	MMLU	IFEval	GSM8K	HumanE.	Average (↑)
Qwen3-0.6B	16-16-16	56.02	34.04	47.23	64.04	67.36	56.04	39.20	31.20	42.84	47.70	40.12	58.41	41.54	37.20	47.35
OmniQuant	4-8-8	48.11	30.46	44.06	66.24	65.07	55.88	37.82	32.00	42.07	48.90	39.11	12.01	0.00	0.00	37.27
OmniQuant	3-8-8	42.42	28.07	38.73	64.19	61.59	54.14	37.15	28.80	43.74	43.81	30.40	11.09	0.00	0.00	34.58
OmniQuant	2-8-8	32.20	21.76	27.66	38.13	54.57	50.28	33.37	26.20	51.43	56.65	22.99	11.65	0.00	0.00	<u>30.49</u>
LQER	4-8-8	55.64	31.83	45.21	63.76	66.05	53.51	38.43	29.80	41.85	47.86	41.13	54.16	31.61	33.54	45.31
LQER	3-8-8	41.33	26.88	39.91	62.05	61.32	52.01	38.18	27.80	43.05	43.52	26.56	38.63	4.32	4.88	36.46
LQER	2-8-8	27.57	25.51	26.74	53.52	53.48	50.36	33.37	27.00	49.98	44.22	23.57	11.09	0.00	0.00	30.46
QuaRot	4-8-8	24.07	27.22	26.59	46.94	51.20	49.64	33.93	29.80	48.25	51.01	24.46	8.50	0.00	0.00	30.12
QuaRot	3-8-8	23.74	27.90	26.40	45.66	51.41	47.59	32.80	29.80	47.47	51.24	25.42	7.95	0.00	0.00	29.81
QuaRot	2-8-8	24.83	27.39	26.25	48.23	51.90	48.38	32.29	30.60	48.85	50.73	24.23	7.95	0.00	0.00	30.12
ABQ-LLM	4-8-8	56.14	34.04	47.46	63.91	67.30	56.83	39.30	31.20	42.76	47.79	40.09	58.04	0.00	38.41	44.52
ABQ-LLM	3-8-8	32.45	23.29	28.43	54.98	54.24	50.36	33.37	25.80	52.50	53.96	23.05	11.65	0.00	0.00	31.72
ABQ-LLM	2.32-8-8	26.18	26.79	26.03	43.00	51.20	49.57	33.98	28.00	49.11	55.29	24.16	12.20	0.00	0.00	30.40
SpinQuant	4-8-8	48.32	30.29	44.41	52.94	65.56	56.27	38.74	32.60	43.42	55.61	32.67	48.61	25.25	3.05	41.27
SpinQuant	3-8-8	40.45	25.77	40.00	38.47	61.15	55.72	37.67	27.80	45.08	56.71	24.36	32.53	3.34	0.00	34.93
SpinQuant	2-8-8	30.77	23.21	27.92	45.47	51.09	50.99	33.83	24.80	43.98	52.44	24.84	11.28	0.00	0.00	30.04
QoQ	4-8-4	24.54	25.09	26.17	39.17	50.82	49.88	32.70	27.00	49.68	56.22	24.95	10.91	0.00	0.00	29.80
FlatQuant	4-8-8	54.21	30.80	45.66	65.87	66.59	56.27	39.61	32.40	44.07	55.92	37.58	55.64	27.14	28.66	<u>45.74</u>
FlatQuant	3-8-8	44.91	28.16	40.17	54.95	62.89	53.43	37.92	28.00	42.20	55.24	31.40	40.11	3.26	0.61	<u>37.38</u>
FlatQuant	2-8-8	28.32	21.84	26.52	39.63	53.37	51.07	34.19	28.20	49.67	56.17	22.94	11.28	0.00	0.00	30.23
EDGE RAZOR	4-8-8	57.79	33.70	45.00	67.49	67.85	55.88	40.17	33.80	43.53	54.09	39.73	53.42	42.00	34.76	47.80
EDGE RAZOR	2.79-8-8	52.10	28.50	37.36	70.58	63.93	53.12	40.12	28.60	42.82	54.97	36.44	49.54	26.99	32.32	44.10
EDGE RAZOR	1.88-8-8	51.47	27.99	34.22	66.85	63.49	53.04	38.02	27.40	43.88	55.92	29.56	44.55	25.09	23.17	41.76
EDGE RAZOR	1.58-8-8	44.87	26.11	33.88	66.73	60.55	51.30	38.28	31.00	44.72	50.76	33.09	38.45	15.01	22.56	39.81

Table 18: Performance of weight-only quantization methods on Qwen3-1.7B across various bit-widths. **Bold** and underlined values indicate the best and second-best average performance.

Models	W-A-KV	ARC-e	ARC-c	HellaS.	BoolQ	PIQA	WinoG.	SIQA	OBQA	TrQA2	Ethics	MMLU	IFEval	GSM8K	HumanE.	Average (↑)
Qwen3-1.7B	16-16-16	69.87	42.83	60.40	77.77	72.58	60.85	45.19	37.40	45.97	49.63	55.49	67.10	68.76	67.07	58.64
GPTQ	4-16-16	62.21	38.40	58.35	76.51	70.35	58.72	42.78	34.80	45.79	55.24	51.37	59.52	59.59	55.49	54.94
GPTQ	3-16-16	56.69	35.15	53.71	69.36	67.08	58.48	41.56	34.80	47.46	51.26	42.03	33.09	9.63	3.66	43.14
GPTQ	2-16-16	25.76	24.91	26.17	48.99	50.27	49.80	33.11	27.80	47.91	51.45	23.54	7.76	0.00	0.00	29.82
OmniQuant	4-16-16	69.11	41.13	58.02	79.79	71.00	62.35	44.63	36.00	44.84	52.10	52.34	15.34	0.00	0.00	44.76
OmniQuant	3-16-16	60.61	36.01	52.49	67.00	68.55	58.33	40.84	32.80	45.24	43.64	48.95	14.60	0.00	0.00	40.65
OmniQuant	2-16-16	40.95	24.32	32.85	59.60	59.19	52.17	35.82	27.40	44.53	44.65	22.94	12.20	0.00	0.00	32.62
AWQ	4-16-16	71.76	43.60	59.71	75.41	71.27	60.46	43.86	36.20	45.66	45.47	54.23	67.84	58.98	62.80	56.95
AWQ	3-16-16	56.36	34.90	52.98	70.52	68.39	58.33	40.02	31.60	45.67	51.45	46.92	48.43	30.10	32.32	47.71
AWQ	2-16-16	25.38	26.54	25.83	62.17	51.41	49.64	32.80	29.60	48.33	43.23	24.65	12.38	0.00	0.00	30.85
AQLM	4-16-16	67.68	42.06	59.84	75.54	71.55	60.69	44.52	36.20	46.08	51.01	55.70	65.25	66.41	63.41	57.57
AQLM	3-16-16	59.01	37.20	55.94	73.85	69.26	59.12	43.14	35.00	43.65	44.94	51.77	53.97	45.34	45.12	51.24
AQLM	2-16-16	55.85	33.11	49.98	67.34	67.08	59.43	42.22	30.80	43.36	43.34	42.81	23.11	21.76	0.00	41.44
BiLLM	1.04-16-16	27.57	27.74	27.49	39.45	50.87	50.91	33.52	25.00	33.52	56.43	25.21	10.35	0.00	0.00	29.15
QuIP#	4-16-16	38.01	23.89	31.36	63.36	58.43	52.57	35.36	25.80	46.91	43.83	24.90	12.94	0.00	0.00	32.67
QuIP#	3-16-16	35.52	22.53	31.51	62.75	56.20	51.85	35.62	26.60	48.15	43.83	28.25	17.56	0.00	0.00	32.88
QuIP#	2-16-16	33.16	20.48	30.02	61.01	54.73	50.59	35.01	24.60	47.81	43.23	24.81	13.12	0.00	0.00	31.33
AutoRound	4-16-16	69.32	43.00	58.88	80.06	70.62	60.62	44.93	36.60	48.53	59.39	55.94	64.70	63.38	60.37	<u>58.31</u>
AutoRound	3-16-16	60.27	37.12	54.62	73.18	69.42	59.75	42.84	35.20	45.44	46.83	49.55	54.90	45.26	46.34	<u>51.48</u>
AutoRound	2-16-16	47.60	28.58	39.78	66.36	61.64	50.83	39.36	30.00	42.59	43.51	30.59	11.83	1.06	0.00	35.27
VPTQ	4-16-16	71.04	39.93	57.55	75.14	70.02	60.22	44.22	35.60	44.21	47.65	54.61	65.25	62.40	63.41	56.52
VPTQ	3-16-16	52.53	37.46	53.75	73.33	68.01	58.88	40.89	35.80	43.39	56.37	36.89	55.45	22.14	29.27	47.44
VPTQ	2-16-16	36.66	25.17	38.08	63.12	58.60	53.91	37.26	28.80	43.36	43.57	25.46	9.80	0.00	0.00	33.13
QTIP	2-16-16	60.14	34.98	53.58	63.61	70.02	58.56	41.50	35.20	43.39	43.42	43.94	44.18	27.37	21.95	<u>45.85</u>
ARB-LLM	1-16-16	31.65	23.21	32.75	62.63	56.42	49.57	35.26	25.00	41.86	44.02	23.22	2.96	0.00	0.00	30.61
GPTAQ	4-16-16	68.52	42.06	58.59	78.72	71.06	59.67	43.45	35.40	46.23	58.34	53.31	63.22	60.96	59.15	57.05
GPTAQ	3-16-16	50.63	31.48	53.95	73.82	69.31	56.91	40.99	34.00	46.53	48.78	41.93	38.45	25.17	10.37	44.45
GPTAQ	2-16-16	28.20	22.27	27.57	43.79	52.72	50.43	34.80	25.40	49.51	53.50	23.52	7.95	0.00	0.00	29.98
Slim-LLM+	3-16-16	61.20	36.35	51.18	68.47	67.79	58.56	41.76	34.60	41.18	44.59	48.60	41.22	35.25	24.39	46.80
Slim-LLM+	2-16-16	34.55	23.55	31.26	61.19	55.93	52.17	35.67	27.80	48.01	44.01	22.95	14.60	0.00	0.00	32.26
Q-Palette	4-16-16	66.25	40.44	58.65	75.44	70.73	61.64	43.09	37.60	44.36	46.37	55.08	33.09	0.00	64.02	49.77
Q-Palette	3.25-16-16	55.68	36.69	56.57	78.35	70.29	57.85	41.04	36.20	46.44	54.30	52.03	29.39	0.00	52.44	47.66
Q-Palette	2-16-16	36.24	24.06	36.09	62.29	59.47	51.78	35.88	27.20	44.39	43.26	25.87	15.71	0.00	0.61	33.06
Q-Palette	1.75-16-16	31.02	22.95	30.28	61.87	54.46	48.38	34.24	23.80	46.96	43.31	22.88	12.75	0.00	0.00	<u>30.92</u>
EDGE RAZOR	4-16-16	70.66	44.80	57.51	80.09	72.31	60.14	44.06	38.40	48.41	64.02	54.70	58.96	68.39	57.32	58.56
EDGE RAZOR	2.79-16-16	63.47	38.57	49.48	78.78	68.23	55.64	43.91	33.40	45.42	60.81	46.25	54.71	54.28	53.66	53.33
EDGE RAZOR	1.88-16-16	59.60	34.04	40.94	72.11	65.23	54.38	41.76	29.80	46.09	57.30	38.93	43.81	36.39	39.63	47.14
EDGE RAZOR																

Table 19: Performance of weight-activation quantization methods on Qwen3-1.7B across various bit-widths. **Bold** and underlined values indicate the best and second-best average performance.

Models	W-A-KV	ARC-e	ARC-c	HellaS.	BoolQ	PIQA	WinoG.	SIQA	OBQA	TrQA2	Ethics	MMLU	IFEval	GSM8K	HumanE.	Average (↑)
Qwen3-1.7B	16-16-16	69.87	42.83	60.40	<u>77.77</u>	72.58	60.85	45.19	37.40	45.97	49.63	55.49	67.10	68.92	67.07	58.65
OmniQuant	4-8-8	67.42	40.36	58.46	76.54	70.57	59.83	44.42	36.80	44.20	47.09	52.96	13.12	0.00	0.00	43.70
OmniQuant	3-8-8	62.21	35.15	52.17	67.74	68.44	56.75	41.71	33.60	44.17	44.65	48.68	14.60	0.00	0.00	40.71
OmniQuant	2-8-8	39.14	22.27	32.91	62.39	58.05	51.22	35.62	28.20	48.22	43.27	22.93	11.65	0.00	0.00	<u>32.56</u>
LQER	4-8-8	66.75	41.38	59.88	71.47	71.60	58.56	42.63	36.40	45.79	45.28	51.67	61.92	59.67	60.98	55.28
LQER	3-8-8	56.82	33.45	52.95	71.62	67.52	56.20	40.74	35.00	45.64	57.30	40.64	43.81	22.74	30.49	46.78
LQER	2-8-8	27.65	24.66	26.56	59.33	50.54	49.57	34.19	25.80	49.68	45.76	22.93	12.20	0.00	0.00	30.63
QuaRot	4-8-8	25.46	26.79	26.63	46.97	51.25	49.64	32.91	29.00	47.71	51.22	24.70	9.98	0.00	0.00	30.16
QuaRot	3-8-8	24.75	26.79	26.43	47.37	50.65	51.85	31.47	30.40	47.13	51.23	24.08	10.17	0.00	0.00	30.17
QuaRot	2-8-8	24.92	26.28	25.87	46.79	51.63	52.33	33.27	27.80	49.13	52.97	24.18	10.35	0.00	0.00	30.39
ABQ-LLM	4-8-8	63.59	40.44	56.43	77.92	70.78	58.64	43.76	35.60	42.25	51.77	52.00	12.94	0.00	0.00	43.29
ABQ-LLM	3-8-8	49.20	30.20	49.25	64.19	65.83	57.46	39.66	33.40	43.27	43.27	41.48	12.20	0.00	0.00	37.82
ABQ-LLM	2.32-8-8	37.37	25.77	28.12	41.01	57.29	52.33	34.95	26.80	47.02	49.66	22.97	11.65	0.00	0.00	31.07
SpinQuant	4-8-8	65.45	39.85	59.25	78.29	71.55	59.75	43.96	38.20	46.09	48.58	54.11	65.06	58.98	57.93	56.22
SpinQuant	3-8-8	60.77	36.60	53.16	76.64	66.54	59.67	40.17	34.40	45.64	55.74	40.75	56.01	26.23	12.80	47.51
SpinQuant	2-8-8	31.73	21.16	31.14	45.35	54.62	48.93	34.75	26.00	45.34	48.59	23.19	3.88	0.00	0.00	29.62
QoQ	4-8-4	24.62	21.50	26.15	37.98	51.74	50.51	33.06	31.20	48.43	56.73	25.50	11.28	0.00	0.00	29.91
FlatQuant	4-8-8	68.01	42.32	58.53	78.13	71.22	59.59	44.11	37.40	47.41	53.19	54.85	66.73	63.23	65.85	57.90
FlatQuant	3-8-8	60.61	36.43	53.47	75.47	67.90	58.33	41.71	34.60	44.70	53.68	47.24	50.28	35.10	28.66	49.16
FlatQuant	2-8-8	26.09	26.54	26.44	39.08	50.05	49.80	33.06	26.40	49.22	56.30	23.61	11.65	0.00	0.00	29.87
EDGERAZOR	4-8-8	70.16	44.45	57.52	79.82	72.58	59.67	43.45	38.20	48.37	63.56	54.29	60.26	68.54	59.15	58.57
EDGERAZOR	2.79-8-8	62.79	38.31	49.53	78.38	68.72	56.04	43.65	33.40	45.57	60.72	46.27	54.34	53.68	50.61	53.00
EDGERAZOR	1.88-8-8	59.09	33.53	40.85	72.14	65.18	53.99	41.76	29.00	46.18	57.33	39.03	41.96	37.53	40.85	47.03
EDGERAZOR	1.58-8-8	55.64	31.48	39.68	70.70	64.25	53.91	41.76	31.60	40.15	56.26	35.07	32.35	28.96	32.93	43.91